

<b>JOURNAL</b>	<i>Cell Host &amp; Microbe</i>
<b>ARTICLE TITLE</b>	IL-9 and mast cells are key players of <i>Candida albicans</i> commensalism and pathogenesis in the gut
<b>AUTHOR LIST</b>	Giorgia Renga, Silvia Moretti, Vasilis Oikonomou, Monica Borghi, Teresa Zelante, Giuseppe Paolicelli, Marco De Zuani, Valeria R. Vilella, Valeria Raia, Rachele Del Sordo, Andrea Bartoli, Monia Baldoni, Jean-Christophe Renaud, Angelo Sidoni, Enrico Garaci, Luigi Maiuri, Carlo E. Pucillo and Luigina Romani
<b>ARTICLE TYPE</b>	Research Article
<b>ABSTRACT</b>	<p><i>Candida albicans</i> is implicated in intestinal diseases. Identifying host signatures that discriminate between the pathogenic vs commensal nature of this human commensal is clinically relevant. In the present study we have identified IL-9 and mast cells (MC) as key players of <i>Candida</i> commensalism and pathogenicity. By inducing TGF-<math>\beta</math> in stromal MC, IL-9 pivotally contributed to mucosal immune tolerance via the indoleamine 2,3-dioxygenase enzyme. However, <i>Candida</i>-driven IL-9 and mucosal MC also contributed to barrier function loss, dissemination and inflammation in experimental leaky gut models and were upregulated in patients with celiac disease. Inflammatory dysbiosis occurred in IL-9 and MC deficiency, a finding indicating that the activity of IL-9 and MC may go beyond host immunity to include regulation of the microbiota. Thus, the output of the IL-9/MC axis is highly contextual during <i>Candida</i> colonization and reveals how host immunity and the microbiota finely tune <i>Candida</i> behavior in the gut.</p>

## **IL-9 and mast cells are key players of *Candida albicans* commensalism and pathogenesis in the gut**

Giorgia Renga<sup>1</sup>, Silvia Moretti<sup>1</sup>, Vasilis Oikonomou<sup>1</sup>, Monica Borghi<sup>1</sup>, Teresa Zelante<sup>1</sup>, Giuseppe Paolicelli<sup>1</sup>, Marco De Zuani<sup>2</sup>, Valeria R. Vilella<sup>3</sup>, Valeria Raia<sup>4</sup>, Rachele Del Sordo<sup>1</sup>, Andrea Bartoli<sup>1</sup>, Monia Baldoni<sup>5</sup>, Jean-Christophe Renaud<sup>6</sup>, Angelo Sidoni<sup>1</sup>, Enrico Garaci<sup>7</sup>, Luigi Maiuri<sup>3,8</sup>, Carlo E. Pucillo<sup>2</sup> and Luigina Romani<sup>1</sup>.

<sup>1</sup>Department of Experimental Medicine, University of Perugia, 06132 Perugia, Italy

<sup>2</sup>Department of Medical and Biological Science, University of Udine, 33100 Udine, Italy

<sup>3</sup>European Institute for Research in Cystic Fibrosis, Division of Genetics and Cell Biology, San Raffaele Scientific Institute, 20132 Milan, Italy

<sup>4</sup>Regional Cystic Fibrosis Center, Pediatric Unit, Department of Translational Medical Sciences, Federico II University Naples 80131, Italy

<sup>5</sup>Department of Medicine, University of Perugia, 06132 Perugia, Italy

<sup>6</sup>Ludwig Institute for Cancer Research, Brussels Branch, B-1200 Brussels, Belgium

<sup>7</sup>San Raffaele Pisana, IRCCS, Telematic University and University of Tor Vergata, 00163 Rome, Italy

<sup>8</sup>Department of Health Sciences, University of Piemonte Orientale, Novara, Italy.

**Running title:** *Candida albicans*, IL-9 and mast cells in the gut

**Keywords:** IL-9, mast cells, *Candida albicans*, intestinal inflammation, IDO1, celiac disease

**Correspondence:** Luigina Romani, M.D., Ph.D.

Department of Experimental Medicine - University of Perugia, Polo Unico Sant'Andrea delle Fratte, 06132 Perugia, Italy

Telephone: +39 075 585 8234

E-mail: [luigina.romani@unipg.it](mailto:luigina.romani@unipg.it)

## SUMMARY

*Candida albicans* is implicated in intestinal diseases. Identifying host signatures that discriminate between the pathogenic vs commensal nature of this human commensal is clinically relevant. In the present study we have identified IL-9 and mast cells (MC) as key players of *Candida* commensalism and pathogenicity. By inducing TGF- $\beta$  in stromal MC, IL-9 pivotally contributed to mucosal immune tolerance via the indoleamine 2,3-dioxygenase enzyme. However, *Candida*-driven IL-9 and mucosal MC also contributed to barrier function loss, dissemination and inflammation in experimental leaky gut models and were upregulated in patients with celiac disease. Inflammatory dysbiosis occurred in IL-9 and MC deficiency, a finding indicating that the activity of IL-9 and MC may go beyond host immunity to include regulation of the microbiota. Thus, the output of the IL-9/MC axis is highly contextual during *Candida* colonization and reveals how host immunity and the microbiota finely tune *Candida* behavior in the gut.

## INTRODUCTION

*Candida albicans* is well adapted for growth in the gastrointestinal tract where the colonization levels reflect an interplay between host immunity, the microbiota and the fungus (Noble et al., 2017; Romani, 2011; Underhill and Pearlman, 2015). Much like antibiotics, intestinal inflammation may perturb the resident bacterial community, creating conditions that favor both high level *Candida* colonization and inflammation. However, despite being implicated in gut immunopathology (Gerard et al., 2015), including celiac disease (CD) (McDermott et al., 2003; Nieuwenhuizen et al., 2003) and sensitization to food antigens (Yamaguchi et al., 2006), *C. albicans* colonization protects against local (Bonifazi et al., 2009; Montagnoli et al., 2002) and distant (Noverr and Huffnagle, 2004) immune pathologies in mice. In humans, the clinical significance of fungi in gastric diseases is still controversial and the need for antifungal therapy has not been reached a consensus (Sasaki, 2012). Thus, identifying host signatures that discriminate between the pathogenic vs protective role of the fungus becomes important.

Recent studies have suggested the possible participation of mast cells (MC) to the *Candida*/host interaction at mucosal surfaces (Lopes et al., 2015; Schlapbach et al., 2014). In vitro, human MC mounted a specific temporal pattern of responses towards *C. albicans* that includes an initial phase characterized by the secretion of granular proteins, neutrophil recruitment and reduced fungal viability followed by a late stage of release of mediators with known anti-inflammatory activity (Lopes et al., 2015). For their strategic location at vascularized mucosal surfaces combined with a unique versatility (Frossi et al., 2017a), MC are well positioned to respond to allergens and pathogens and modulate mucosal immune responses (Abraham and St John, 2010; Reber et al., 2015), thus contributing to a wide variety of human infections and diseases (Frossi et al., 2017a). Phenotypic and functional characteristics of MCs can be tuned by many genetic and environmental factors, including changes in the cytokine milieu associated with inflammatory or immune responses (Frossi et al.,

2017a; Galli et al., 2005). However, despite their potential phenotypic “plasticity”, two types of MC have been described in mice based on their protease content and location: “connective tissue-type” MC (CTMC), derived from fetal liver progenitors and primarily located in stromal tissue and mucosal MC (MMC) of bone marrow origin and residing in the gut and lung (Gurish and Austen, 2012; Reber et al., 2015).

Among MMC, IL-9-producing mucosal MC (MMC9) are the principal producers of IL-9 (~2.0 pg/ml per cell) (Chen et al., 2015), the key cytokine that autocrinally drives mastocytosis (Renauld et al., 1990). MMC9s are scarce in the small intestines of immunologically naïve mice and expand considerably after repeated ingested antigen exposure (Chen et al., 2015). In addition to MMC9, innate lymphoid (ILC)2 and Th9 cells may also serve as alternative cellular sources of IL-9, thus amplifying intestinal mastocytosis involved not only in food allergy and systemic anaphylaxis (Chen et al., 2015; Shik et al., 2017) but also in intestinal inflammation (Boeckxstaens, 2015; Gerlach et al., 2014; Nalleweg et al., 2015) and in the onset and progression of CD (Frossi et al., 2017b). Yet, several lines of evidence show that MC and IL-9 may also suppress chronic inflammatory responses and promote immune tolerance (de Vries and Noelle, 2010; Lu et al., 2006; Metz et al., 2007). Thus, by integrating multiple signals and mechanisms, MC promote either inflammatory immunity or immune tolerance.

It has recently been reported that the MC-ILC2-Th9 pathway exacerbates aspergillosis and promotes lung inflammation in cystic fibrosis (CF) (Moretti et al., 2017). In candidiasis, Th9 responses were defective in patients with Chronic Mucocutaneous Candidiasis (Becker et al., 2016), and abundant in *Candida*-driven skin inflammation (Schlapbach et al., 2014). Thus, a role for the IL-9/MC axis in mucosal candidiasis is plausible but never been directly demonstrated. In the present study, we have revealed that IL-9 and MC are key players of *Candida* pathogenicity at mucosal surfaces. By inducing the indoleamine 2,3-dioxygenase enzyme in response to the fungus, IL-9 pivotally contributed to local immune tolerance. However, IL-9 and mucosal MC also contributed to barrier function loss, dissemination and inflammation in experimental models of impaired intestinal barrier function and were upregulated in patients with celiac disease. Inflammatory dysbiosis occurred in the relative absence of IL-9 and MC, a finding indicating that the activity of IL-9 and MC may go beyond host immunity to include regulation of the microbiota.

## RESULTS

### **The IL-9/IL-9R signaling pathway promotes innate and Th immunity to *C. albicans***

We resorted to primary and secondary gastrointestinal infections in C57BL/6 and *I19R*<sup>-/-</sup> mice to measure IL-9 production and *I19R* expression in infection. Increased production of IL-9 and expression of *I19R* were observed in the stomach of C57BL/6 but not *I19R*<sup>-/-</sup> mice (Figure 1A and B), a finding suggesting that IL-9 production is IL-9R-dependent. Both innate and adaptive immune responses contributed to IL-9 production, as indicated by the high levels observed early and late in infection and the defective production in *Rag2*<sup>-/-</sup>*I19R*<sup>-/-</sup> (Figure S1A).

IL-9 production was not defective in IL-4 or IL-17RA deficient mice (Figure S1A), which finding indicates that Th2 and Th17 cells do not contribute to IL-9 production, as suggested (Kaplan, 2013). Increased production of IL-9 was also observed in the ileum (from  $20 \pm 3$  to  $300 \pm 13$  pg/ml, naïve vs 3-day infected mice) and colon (from  $76 \pm 6$  to  $540 \pm 33$  pg/ml, naïve vs 3-day infected mice).

ILC2, MMC9 and Th9 are the most potent producers of IL-9 at mucosal surfaces (Kaplan, 2013; Wilhelm et al., 2011). We found that the *Rora* transcription factor of ILC2, the *Pu.1* and *Irf4* transcription factors of Th9 (Figure 1C) were lower in *Il9R<sup>-/-</sup>* than C57BL/6 mice. Consistent with the significant reduction of IL-9 levels in MC-deficient C57BL/6-Kit<sup>W/W<sup>v</sup></sup> (hereafter indicated as Kit<sup>W/W<sup>v</sup></sup>) (Figure 1A), the production of the MC protease (MCPT)-1 (Figure 1D) was also lower in *Il9R<sup>-/-</sup>* than C57BL/6 mice. *Gata3* and *Foxp3*, but not *Tbet* or *Rorc*, also failed to up-regulate in *Il9R<sup>-/-</sup>* mice during infection (Figure 1E). Together with the lower production of the neutrophil chemoattractant, KC, and inflammatory TNF- $\alpha$ , IL-17A and IL-1 $\beta$ , cytokines observed in *Il9R<sup>-/-</sup>* than C57BL/6 mice (Figure 1F), this immune profile would predict an impact of the defective IL-9/IL-9R signaling on the course of the infection. This appeared to be the case as the loss of IL-9R signaling led to reduced inflammatory cell recruitment in the stomach (Figure 1G) and colon (inset of Figure 1G) and, paradoxically, reduced local fungal growth, particularly early in the course of the infection (Figure 1H). Similar results were obtained in *Rag2<sup>-/-</sup>Il9R<sup>-/-</sup>* (Figure S1), thus suggesting that defective IL-9R signaling in innate cells contributes to the increased resistance. Importantly, IL-9 ablation by means of neutralizing antibody and exogenous IL-9 administration increased or decreased, respectively, resistance to infection, as indicated by the local fungal growth (Figure 1I) and pattern of inflammatory cytokine production (Figure 1J), thus suggesting the causal role of IL-9 in impairing early antifungal resistance. All together, these results suggest that the IL-9/IL-9R signaling is dispensable for resistance, if not contributing to pathogenic inflammation, during the initial *C. albicans* infection.

Surprisingly, the effects of IL-9 ablation or administration were different late in infection, at the time at which resistance to infection was instead promoted by IL-9 and impaired upon IL-9 inhibition. On testing the hypothesis of a possible disparate activity of IL-9 on innate and adaptive immunity to the fungus, we assessed *Il9R<sup>-/-</sup>* mice for resistance to re-infection and parameters of adaptive Th immunity. *Il9R<sup>-/-</sup>* mice were less resistant than C57BL/6 mice to re-infection, as indicated by the decreased survival (Figure 2A), the inability to control fungal dissemination despite a degree of control of the fungal growth locally (Figure 2B) and the increased inflammatory pathology both in the stomach and the kidneys (Figure 2C). IL-9 production and Th9 cell were expectedly lower in *Il9R<sup>-/-</sup>* than C57BL/6 mice (Figure 2D). In contrast, Th1/Th17 cell activation was higher, but Treg cell activation lower, and Th2 apparently unaffected, in *Il9R<sup>-/-</sup>* than C57BL/6 mice (Figure 2E), a finding pointing to dysfunctional Th responses in condition of IL-9R deficiency that could account for the failure to mount memory responses to the fungus (Montagnoli et al., 2002). All together, these results suggest a temporal distinct activity of IL-9 in infection, being required for optimal Th/Treg-mediated protection but dispensable for innate antifungal defense.

## The IL-9/IL-9R signaling pathway regulates MC activity in infection

The above results prompted us to investigate mechanisms behind the opposite activity of IL-9 in infection and re-infection. Given the ability of IL-9 to inhibit the oxidative burst of effector phagocytes (Pilette et al., 2002), IL-9 could adversely affect the activity of effector phagocytes. Although IL-9 slightly decreased the oxidative burst and the candidacidal activity in vitro (Figure S2), the antifungal activity was not impaired in *Il9R<sup>-/-</sup>* mice (Figure S2). Thus, the reduced inflammatory response of *Il9R<sup>-/-</sup>* mice was not secondary to a reduced fungal growth. To unravel mechanisms uncoupling the inflammatory response from the fungal growth, we looked for MC expansion and activity in infection, considering that MC promote neutrophil recruitment (Malaviya et al., 1996), regulate acquired immune responses (Galli et al., 2005) and are directly responsible for increasing epithelial paracellular permeability during intestinal infections via MCPT-1 (McDermott et al., 2003). MC expanded early in the forestomach and glandular stomach of C57BL/6 but not *Il9R<sup>-/-</sup>* mice to decline thereafter (from  $1.83 \pm 0.26$  MC/mm<sup>2</sup> in uninfected mice to  $3.50 \pm 0.70$  and  $2.40 \pm 0.40$ , at 3 and 10 dpi, respectively), as seen by toluidine blue staining (Figure S3). Of interest, safranin-negative/alcian blue-positive MC were localized in the mucosa early in infection while alcian-blue negative/safranin-positive MC were continuously present in the connective tissue, indicating that both MMC and CTMC, respectively, expanded in infection (Figure 3A). This finding is consistent with the pattern of specific MC proteases gene expression, showing the peak expression of the MMC-related chymase, *Mcpt1*, at 3 days (Figure 3B) and the expression of the CTMC-related chymase, *Mcpt4*, and tryptase, *Mcpt6*, continuously present through the infection (Figure 3B).

To functionally characterize the MC subtypes, we cultivated bone marrow (BM)-derived MC in the presence of IL-3, alone or with stem cell factor, to obtain MC considered to be the tissue culture equivalent of MMC or CTMC, respectively (Godfraind et al., 1998). We stimulated MC subtypes with *Candida* and/or IgE/Ag and looked for degranulation, phagocytosis and killing of the fungus and cytokine production. Consistent with the ability of the fungus to degranulate human MC at high multiplicity of infection only (Lopes et al., 2015), degranulation was not induced, if not inhibited, in either MC subtype in response to *Candida* yeasts or hyphae (Figure 3C). MC subtypes, despite being able to phagocytose unopsonized yeasts but not hyphae, exhibited different candidacidal activity, being MMC unable to kill the ingested fungi (Figure 3D), as suggested (Trevisan et al., 2014). Actually the massive MCPT-1 release would suggest MMC's necrosis, an effect potentiated by IL-9 (Figure 3E). Killing of the ingested yeasts (Figure 3D) and no release of MCPT-1 (Figure 3E) was instead observed with CTMC. MC discriminated between the fungal morphotypes in terms of TGF- $\beta$  and IL-10 production, being CTMC, more than MMC, able to release both cytokines in response to hyphae, a release again potentiated by IL-9 (Figure 3F). Either MC subtype produced IL-9 in response to *Candida* (Fig. 3F), and no differences were observed in *Il1b* and *Tnfa* gene expression in either MC subtype (data not shown). These findings indicate that *C. albicans* exploits the MC's functional versatility at mucosal surfaces to contribute to local damage and inflammation or protection.

## **IL-9 and MMC affect intestinal epithelial permeability and adaptive immunity**

The effect of IL-9 on MCPT1 production would predict an impact on epithelial cell permeability. We used dextran-FITC to detect leakage in the early stages of permeability induction. Leakage was observed at 3 dpi in C57BL/6 mice and was dependent on both IL-9 and MC, as evidenced by the reduced leakage in *Il9R<sup>-/-</sup>* or *Kit<sup>W/W-v</sup>* mice and its promotion upon IL-9 administration together with engrafted BMDC in MC-deficient mice (Figure 4A). Consistent with the up-regulated expression of the sealing protein occludin in the colon of *Il9<sup>-/-</sup>* mice (Gerlach et al., 2015), occludin expression was up-regulated in *Il9R<sup>-/-</sup>* or *Kit<sup>W/W-v</sup>* mice and down-regulated in C57BL/6 mice (Figure 4B). Paralleling the pattern of epithelial permeability, *Candida* dissemination also occurred (Figure 4C), a finding that prompted us to assess whether MC also regulate systemic adaptive immunity to the fungus. To this purpose, we subjected *Kit<sup>W/W-v</sup>* mice to the primary or secondary gastrointestinal infection with *C. albicans*. The inflammatory response was reduced in these mice as compared to C57BL/6 mice in the early phase of the infection, both in terms of inflammatory cells recruitment (Figure 4D), local fungal growth (Figure 4E) and *Tnfa* and *Il1b* gene expression (Figure 4F). In contrast, *Kit<sup>W/W-v</sup>* mice failed to control both the inflammatory pathology (Figure 4D) and the fungal growth (Figure 4E) upon re-infection, and to activate memory protective Th1/Treg cell responses (Figure 4G). These results highlight the potent immunomodulatory role of MC that both augment (Shelburne et al., 2009) and regulate the quality (Mekori et al., 2016) of the adaptive immunity. All together, these findings point to an IL-9/MDC-dependent negative activity on intestinal permeability that may account for inflammation, *Candida* dissemination and dysregulated Th immunity.

## **IL-9 regulates indoleamine 2,3-dioxygenase (IDO)1 activity**

TGF- $\beta$  is known to provide long-term immune tolerance by regulating the activity of IDO1 (Pallotta et al., 2011) known to be crucially involved in Treg-mediated memory responses to the fungus (De Luca et al., 2007; Montagnoli et al., 2002). Thus, the defective expansion of TGF- $\beta$ -producing CTMC in *Il9R<sup>-/-</sup>* mice would predict a defective IDO1 activity in these mice. IDO1 expression was indeed defective in infection and particularly in re-infection in *Il9R<sup>-/-</sup>* mice as opposed to C57BL/6 mice (Figure 5A and B) and paralleled the decreased production of TGF- $\beta$  observed in *Il9R<sup>-/-</sup>* and *Kit<sup>W/W-v</sup>* mice (Figure 5C). The decreased expression of *Ptpn6* (coding for SHP-1) (Figure 5D) testified functional TGF- $\beta$  deficiency for long term tolerance (Pallotta et al., 2011). This finding suggests that IL-9 may regulate IDO1 activity via MC-dependent TGF- $\beta$  production. This appeared to be the case as IL-9 activated *Tgfb*, *Ptpn6* and *Indo1* gene expression (Figure 5E) and STAT3/IDO1 phosphorylation on splenic dendritic cells at the optimal concentrations ranging from 10 to 100 ng/ml (Figure 5F). Thus, IL-9 appears to act as a potent regulator of IDO1 activity via transcriptional and post-transcriptional mechanisms. Of great interest, IL-9 also mediated IDO1 phosphorylation induced by the fungus, as indicated by the defective phosphorylation observed in the presence of IL-9-neutralizing antibody (Figure

5F). All together, our results offer a plausible explanation for the dual role for IL-9 in *C. albicans* colonization. IL-9 negatively impacted on innate antifungal resistance by expanding inflammatory MMC eventually leading to barrier function loss; however, it was required for the activation of optimal antifungal Th/Treg response by promoting IDO1 activity with the contribution of CTMC producing TGF- $\beta$ . However, MC are known to mediate immune suppression also via Tph-1 (tryptophan hydroxylase-1), a synthase which catalyses the conversion of tryptophan to serotonin (Nowak et al., 2012). On assessing the possible contribution of Tph-1, we found that CTMC and not MMC express *Tph1* (Figure 5G) and *Tph1* expression was lower in *Il9R*<sup>-/-</sup> than C57BL/6 mice (Figure 5G). Consistent with the tolerogenic potential of Tph-1, inflammation (Figure 5H) and fungal growth (Figure 5I) were increased while tolerance decreased (Figure 5J) in *Tph1*<sup>-/-</sup> mice. Thus, CTMC may concur to ensure tolerance at the host/*Candida* interface through multiple mechanisms.

### **IL-9 and MC affect gut microbial composition**

Given the ability of the IL-9/MC axis to promote either inflammation or immune tolerance in the gut, we searched for qualitative and/or quantitative changes in gut bacterial communities in *Candida*-infected mice. Firmicutes, abundantly present in *Il9R*<sup>-/-</sup> and *Kit*<sup>W/W<sup>v</sup></sup> mice, further expanded in infection in these mice as well as in C57BL/6 mice (Figure 6A) with *Lactobacillaceae* more than *Clostridiaceae* expanded in C57BL/6 and *Il9R*<sup>-/-</sup> mice and *Clostridiaceae* more than *Lactobacillaceae* expanded in *Kit*<sup>W/W<sup>v</sup></sup> mice (Figure 6A). Bacteroidetes and *Prevotellaceae* expanded in C57BL/6 and particularly in *Kit*<sup>W/W<sup>v</sup></sup> mice, while Proteobacteria and *Enterobacteriaceae* expanded in *Kit*<sup>W/W<sup>v</sup></sup> mice late in infection (Figure 6A). Of interest, *L. johnsonii* was abundant in both C57BL/6 and *Il9R*<sup>-/-</sup> mice, but *L. reuteri* was expanded in *Il9R*<sup>-/-</sup> mice either uninfected or in infection (Figure 6B). Consistent with the ability of this Lactobacillus strain to activate colonization resistance via the AhR/IL-22 axis involving ILC3 (Zelante et al., 2013), local Ror $\gamma$ <sup>+</sup>CD127<sup>+</sup>ILC3 were expanded (Figure 6C), *AhR* expression and IL-22 production (Figure 6D) and *Lcn2* expression (Figure 6E) were all increased in *Il9R*<sup>-/-</sup> mice. Microbiota transplantation between C57BL/6 and *Il9R*<sup>-/-</sup> mice revealed that antifungal resistance was increased and inflammation decreased in C57BL/6 receiving fecal content from *Il9R*<sup>-/-</sup> mice, while the opposite occurred in *Il9R*<sup>-/-</sup> mice transplanted with C57BL/6 feces (Figure 6F-H). This point to the contribution of local microbiota to antifungal resistance and mucosal homeostasis in condition of IL-9, and likely, MC deficiency, a finding also confirmed by the increased inflammatory pathology observed upon antibiotic treatment (Figure S4A-C). However, the late expansion of Proteobacteria in *Kit*<sup>W/W<sup>v</sup></sup> mice suggests the unique ability of MC to affect the microbial composition via inflammation-driven dysbiosis (Stecher, 2015).

## IL-9 and MMC are up-regulated in experimental leaky gut models and CD patients

To accommodate the above findings in a clinically relevant setting, we evaluated the presence of IL-9 and MC in experimental models of impaired barrier function, such as in homozygous *F508del-Cftr* C57BL/6 mice (*Cftr*<sup>F508del/F508del</sup>, hereafter referred to as *Cftr*<sup>F508del</sup> mice) with gastrointestinal candidiasis or mice with gluten sensitivity (Papista et al., 2012) as well as in duodenal biopsies from CD patients, scored according to the Marsh classification modified by Oberhuber (Institute, 2006; Oberhuber et al., 1999). *Cftr*<sup>F508del</sup> mice, while highly susceptible to *C. albicans* gastrointestinal infection in terms of fungal growth and inflammatory pathology (Figure S5), showed an increased production of IL-9 (Figure 7A), increased *Pu.1* and *Irf4* expression (Figure 7B), and increased MMC activity (Figure 7C). Consistent with the remarkable fungal dissemination to visceral organs (Figure S5), occludin expression was decreased in these mice (Figure 7D), a finding suggesting an impaired intestinal permeability. IL-9 production (Figure 7E), *Pu.1* and *Irf4* expression (Figure 7F) and MMC activity (Figure 7G) were also all increased in gluten-sensitive mice along with a decreased occludin expression (Figure 7H). Similarly, IL-9 positivity was increased in the duodenal biopsies from CD patients, correlated positively with the infiltration of CD3<sup>+</sup> T cells, CD117<sup>+</sup>, tryptase<sup>+</sup> MC and disease severity and negatively with IDO1 expression (Figure 7I and Figure S6). Thus, the IL-9/MMC expansion is a distinctive feature of disease severity in murine models of leaky gut, such as in the CF gut, gluten sensitivity and human CD.

## DISCUSSION

This study shows a plausible mechanism by which *C. albicans* could promote either immune pathology or protective tolerance in the gut. That MC and IL-9 are associated with intestinal diseases, from food allergy (Chen et al., 2015; Forbes et al., 2008) to inflammation (Boeckxstaens, 2015; Gerlach et al., 2014; Nalleweg et al., 2015; Weigmann and Neurath, 2017) is well known. However, that *C. albicans* was able to exploit the versatility of the IL-9/MC axis for balancing commensalism vs pathogenesis is a novel finding. Consistent with the ability of MC to respond to pathogens via Toll-like receptors (Abraham and St John, 2010), recognition of the fungus by MC was dependent on fungal morphotype and MC subtype, with hyphae promoting anti-inflammatory cytokine production by CTMC and yeasts MMC's death and damage. IL-9 pivotally contributed to the discriminative responses of MC. Produced by MMC9, in addition to ILC2 and Th9 cells, IL-9 stimulated secretion of proteases and cytokine, including its own, by both MC subtypes. A positive amplification loop between ILC2 producing IL-9 and MMC9 likely maximizes IL-9 production and promotes epithelial damage and inflammation. Thus, while exerting divergent antifungal effector activity, the different MC, finely tuned by IL-9, appears to discriminate between fungal morphotypes and, in so doing, promote basal immune tolerance or epithelial damage.

Although the small intestine is usually considered the primary site of uptake of food antigens (Walker et al., 1972), uptake of food antigens can also occur in the stomach (Hatz et al., 1990). Therefore, *C. albicans* colonization of the stomach where mastocytosis occurred could be associated with barrier function loss, a

finding suggesting a possible pathogenic role of the fungus in the development of gastric diseases. At variance with known risk factors favoring fungal colonization in the stomach (Scott and Jenkins, 1982), epithelial damage promoted through MMC activation could be the key event promoting transition from fungal commensalism to pathogenesis, as already suggested (Moyes et al., 2016). Given the inflammatory activity of *C. albicans*-specific Th9 cells in the skin (Schlapbach et al., 2014), a pathogenic role for Th9 is also plausible. However, we found that Th9 cells are dispensable for immune pathology and are not detected in condition of failure to activate Treg cells, a finding in line with the functional plasticity of Th9 cells capable of exerting protective and pathogenic roles in different clinical setting (Elyaman et al., 2009; Schmitt et al., 2014). It is intriguing that a sex dimorphism at IL9 and IL9R loci (Schuurhof et al., 2010) increased the risk of *Aspergillus* allergy in female more than male (Moretti et al., 2017). Should this risk extends to *Candida* allergy, this would be in line with the increased resistance to mucosal candidiasis (including the vaginal infection, Figure S7) observed in *IL9R*<sup>-/-</sup> mice and predict an increased risk of candidiasis in carriers of this polymorphism.

The above results confirm the patho-inflammatory role of the IL-9/MC pathway in CF (Moretti et al., 2017) and suggest that the IL-9/MC axis could be an attractive drugable pathway to prevent the clinical unwanted consequences of fungal colonization. However, the occurrence of *Candida* pneumonia in patients receiving imatinib mesylate treatment suggests that MC-targeted therapy might predispose patients to opportunistic and life-threatening fungal infections (Speletas et al., 2008). This study provides a plausible explanation for MC-mediated protection. Consistent with their immunoregulatory role on adaptive immune responses (Morita et al., 2016), tissue remodeling, homeostasis and peripheral tolerance (Galli et al., 2008; Lu et al., 2006), CTMC greatly contributed to the activation of intestinal immune tolerance via Tph1 and IDO1. That MC transactivate IDO1 in DC has been already described (Rodrigues et al., 2016). Here we found that IL-9 may not only directly affect IDO1 gene expression, via STAT3 (Demoulin et al., 1999) in MC, but also promote IDO1-long term tolerance via TGF- $\beta$  (Pallotta et al., 2011). Together with IL-4, TGF- $\beta$  is able to promote Th9 cell development *in vitro* (Goswami et al., 2012), a finding highlighting the potential role of TGF- $\beta$  in reinforcing Th9 activity *in vivo*. Interestingly, TGF- $\beta$  production by MC in response to IL-9 promotes lung fibrosis in aspergillosis (Moretti et al., 2017), a finding suggesting that modules of effector immunity may have different functional outcome contingent upon the context.

Tryptophan abundance in condition of defective host IDO1 expression is known to expand *L. reuteri* that provides colonization resistance to *Candida* via the AhR/ILC3/IL-22 axis (Zelante et al., 2013). All these microbial signatures were present in *IL9R*<sup>-/-</sup> mice and were responsible for the decreased inflammatory pathology and increased antifungal resistance, as demonstrated by the fecal microbiota transplant experiment. Thus, the microbiota provides antifungal resistance in condition of IL-9 deficiency much like in IDO1 deficiency. However, one most interesting, and yet unexplained, finding, is the failure of the microbiota to provide antifungal resistance in re-infection, which suggests that a dysregulated adaptive immunity affects the function of the microbiota. It is also likely that the activity of the adaptive immunity encompasses an effect on MC

plasticity (Daeron, 2016), including the ability of MC to act as intestinal sensors of local microbiota. We found indeed a unique pattern of intestinal dysbiosis in MC-deficient mice in which *Clostridiaceae* and *Enterobacteriaceae* expanded early and late, respectively, during *Candida* colonization, thus suggesting a specific temporal pattern of MC-dependent regulation of local microbial composition. How nutrient availability, promotion of inflammation or lack of tolerance contribute to microbial sensing and regulation by MC at mucosal surfaces remained to be determined. Dysbiosis is a known risk factor for CD (Girbovan et al., 2017) and intestinal inflammation in CF (Garg and Ooi, 2017), conditions in which persistent symptoms are associated with a higher relative abundance of Proteobacteria and a lower abundance of Bacteroidetes and Firmicutes. This study provide evidence that the relative high levels of IL-9 and MMC observed in biopsies from patients with CD may promote an inflammation-driven intestinal dysbiosis to which tryptophan deficiency may contribute. Thus, the IL-9/MC axis, by integrating signals derived from the perturbed host/microbiota homeostasis, may act as signatures that discriminate between the pathogenic vs protective role of the fungus in the gut.

#### **AUTHOR CONTRIBUTIONS**

G.R. and V.O. designed the experiments and performed most of the in vitro and in vivo experiments; M.B. performed immunofluorescence experiments; T.Z., G.P. and M.D.Z. performed experiments with mastocytes; V.R.V performed experiments in gluten-sensitive mice; V.R., R.D.S., M.B. and A.S. followed patients and provided clinical samples; J.C.R. provided the knock out mice; A.B., S.M., E.G., L.M., C.E.P. and L.R. designed the experiments, analyzed the data and wrote the paper.

#### **ACKNOWLEDGMENT**

This study was supported by the Specific Targeted Research Project FunMeta (ERC-2011-AdG-293714 to LR).

## References

- Abraham, S.N., and St John, A.L. (2010). Mast cell-orchestrated immunity to pathogens. *Nat Rev Immunol* 10, 440-452.
- Becker, K.L., Rosler, B., Wang, X., Lachmandas, E., Kamsteeg, M., Jacobs, C.W., Joosten, L.A., Netea, M.G., and van de Veerdonk, F.L. (2016). Th2 and Th9 responses in patients with chronic mucocutaneous candidiasis and hyper-IgE syndrome. *Clin Exp Allergy* 46, 1564-1574.
- Boeckxstaens, G. (2015). Mast cells and inflammatory bowel disease. *Curr Opin Pharmacol* 25, 45-49.
- Bonifazi, P., Zelante, T., D'Angelo, C., De Luca, A., Moretti, S., Bozza, S., Perruccio, K., Iannitti, R.G., Giovannini, G., Volpi, C., *et al.* (2009). Balancing inflammation and tolerance in vivo through dendritic cells by the commensal *Candida albicans*. *Mucosal Immunol* 2, 362-374.
- Chen, C.Y., Lee, J.B., Liu, B., Ohta, S., Wang, P.Y., Kartashov, A.V., Mugge, L., Abonia, J.P., Barski, A., Izuhara, K., *et al.* (2015). Induction of Interleukin-9-Producing Mucosal Mast Cells Promotes Susceptibility to IgE-Mediated Experimental Food Allergy. *Immunity* 43, 788-802.
- Daeron, M. (2016). Innate myeloid cells under the control of adaptive immunity: the example of mast cells and basophils. *Curr Opin Immunol* 38, 101-108.
- De Luca, A., Montagnoli, C., Zelante, T., Bonifazi, P., Bozza, S., Moretti, S., D'Angelo, C., Vacca, C., Boon, L., Bistoni, F., *et al.* (2007). Functional yet balanced reactivity to *Candida albicans* requires TRIF, MyD88, and IDO-dependent inhibition of Rorc. *J Immunol* 179, 5999-6008.
- de Vries, V.C., and Noelle, R.J. (2010). Mast cell mediators in tolerance. *Curr Opin Immunol* 22, 643-648.
- Demoulin, J.B., Van Roost, E., Stevens, M., Groner, B., and Renauld, J.C. (1999). Distinct roles for STAT1, STAT3, and STAT5 in differentiation gene induction and apoptosis inhibition by interleukin-9. *J Biol Chem* 274, 25855-25861.
- Elyaman, W., Bradshaw, E.M., Uyttenhove, C., Dardalhon, V., Awasthi, A., Imitola, J., Bettelli, E., Oukka, M., van Snick, J., Renauld, J.C., *et al.* (2009). IL-9 induces differentiation of TH17 cells and enhances function of FoxP3+ natural regulatory T cells. *Proc Natl Acad Sci U S A* 106, 12885-12890.
- Forbes, E.E., Groschwitz, K., Abonia, J.P., Brandt, E.B., Cohen, E., Blanchard, C., Ahrens, R., Seidu, L., McKenzie, A., Strait, R., *et al.* (2008). IL-9- and mast cell-mediated intestinal permeability predisposes to oral antigen hypersensitivity. *J Exp Med* 205, 897-913.
- Frossi, B., Mion, F., Tripodo, C., Colombo, M.P., and Pucillo, C.E. (2017a). Rheostatic Functions of Mast Cells in the Control of Innate and Adaptive Immune Responses. *Trends Immunol.*
- Frossi, B., Tripodo, C., Guarnotta, C., Carroccio, A., De Carli, M., De Carli, S., Marino, M., Calabro, A., and Pucillo, C.E. (2017b). Mast cells are associated with the onset and progression of celiac disease. *J Allergy Clin Immunol* 139, 1266-1274 e1261.
- Galli, S.J., Grimaldeston, M., and Tsai, M. (2008). Immunomodulatory mast cells: negative, as well as positive, regulators of immunity. *Nat rev Immunol* 8, 478-486.
- Galli, S.J., Kalesnikoff, J., Grimaldeston, M.A., Piliponsky, A.M., Williams, C.M., and Tsai, M. (2005). Mast cells as "tunable" effector and immunoregulatory cells: recent advances. *Annu Rev Immunol* 23, 749-786.

- Garg, M., and Ooi, C.Y. (2017). The Enigmatic Gut in Cystic Fibrosis: Linking Inflammation, Dysbiosis, and the Increased Risk of Malignancy. *Curr Gastroenterol Rep* 19, 6.
- Gerard, R., Sendid, B., Colombel, J.F., Poulain, D., and Jouault, T. (2015). An immunological link between *Candida albicans* colonization and Crohn's disease. *Crit Rev Microbiol* 41, 135-139.
- Gerlach, K., Hwang, Y., Nikolaev, A., Atreya, R., Dornhoff, H., Steiner, S., Lehr, H.A., Wirtz, S., Vieth, M., Waisman, A., *et al.* (2014). TH9 cells that express the transcription factor PU.1 drive T cell-mediated colitis via IL-9 receptor signaling in intestinal epithelial cells. *Nat Immunol* 15, 676-686.
- Gerlach, K., McKenzie, A.N., Neurath, M.F., and Weigmann, B. (2015). IL-9 regulates intestinal barrier function in experimental T cell-mediated colitis. *Tissue Barriers* 3, e983777.
- Girbovan, A., Sur, G., Samasca, G., and Lupan, I. (2017). Dysbiosis a risk factor for celiac disease. *Med Microbiol Immunol* 206, 83-91.
- Godfraind, C., Louahed, J., Faulkner, H., Vink, A., Warnier, G., Grecis, R., and Renaud, J.C. (1998). Intraepithelial infiltration by mast cells with both connective tissue-type and mucosal-type characteristics in gut, trachea, and kidneys of IL-9 transgenic mice. *J Immunol* 160, 3989-3996.
- Goswami, R., Jabeen, R., Yagi, R., Pham, D., Zhu, J., Goenka, S., and Kaplan, M.H. (2012). STAT6-dependent regulation of Th9 development. *J Immunol* 188, 968-975.
- Gurish, M.F., and Austen, K.F. (2012). Developmental origin and functional specialization of mast cell subsets. *Immunity* 37, 25-33.
- Hatz, R.A., Bloch, K.J., Harmatz, P.R., Gonnella, P.A., Ariniello, P.D., Walker, W.A., and Kleinman, R.E. (1990). Divalent hapten-induced intestinal anaphylaxis in the mouse enhances macromolecular uptake from the stomach. *Gastroenterology* 98, 894-900.
- Institute, A.G.A. (2006). AGA Institute Medical Position Statement on the Diagnosis and Management of Celiac Disease. *Gastroenterology* 131, 1977-1980.
- Kaplan, M.H. (2013). Th9 cells: differentiation and disease. *Immunol rev* 252, 104-115.
- Lopes, J.P., Stylianou, M., Nilsson, G., and Urban, C.F. (2015). Opportunistic pathogen *Candida albicans* elicits a temporal response in primary human mast cells. *Sci Rep* 5, 12287.
- Lu, L.F., Lind, E.F., Gondek, D.C., Bennett, K.A., Gleeson, M.W., Pino-Lagos, K., Scott, Z.A., Coyle, A.J., Reed, J.L., Van Snick, J., *et al.* (2006). Mast cells are essential intermediaries in regulatory T-cell tolerance. *Nature* 442, 997-1002.
- Malaviya, R., Ikeda, T., Ross, E., and Abraham, S.N. (1996). Mast cell modulation of neutrophil influx and bacterial clearance at sites of infection through TNF-alpha. *Nature* 381, 77-80.
- McDermott, J.R., Bartram, R.E., Knight, P.A., Miller, H.R., Garrod, D.R., and Grecis, R.K. (2003). Mast cells disrupt epithelial barrier function during enteric nematode infection. *Proc Natl Acad Sci U S A* 100, 7761-7766.
- Mekori, Y.A., Hershko, A.Y., Frossi, B., Mion, F., and Pucillo, C.E. (2016). Integrating innate and adaptive immune cells: Mast cells as crossroads between regulatory and effector B and T cells. *Eur J Pharmacol* 778, 84-89.
- Metz, M., Grimbaldston, M.A., Nakae, S., Piliponsky, A.M., Tsai, M., and Galli, S.J. (2007). Mast cells in the promotion and limitation of chronic inflammation. *Immunol rev* 217, 304-328.

- Montagnoli, C., Bacci, A., Bozza, S., Gaziano, R., Mosci, P., Sharpe, A.H., and Romani, L. (2002). B7/CD28-dependent CD4+CD25+ regulatory T cells are essential components of the memory-protective immunity to *Candida albicans*. *J Immunol* *169*, 6298-6308.
- Moretti, S., Renga, G., Oikonomou, V., Galosi, C., Pariano, M., Iannitti, R.G., Borghi, M., Puccetti, M., De Zuani, M., Pucillo, C.E., *et al.* (2017). A mast cell-ILC2-Th9 pathway promotes lung inflammation in cystic fibrosis. *Nat Commun* *8*, 14017.
- Morita, H., Saito, H., Matsumoto, K., and Nakae, S. (2016). Regulatory roles of mast cells in immune responses. *Semin Immunopathol* *38*, 623-629.
- Moyes, D.L., Wilson, D., Richardson, J.P., Mogavero, S., Tang, S.X., Wernecke, J., Hofs, S., Gratacap, R.L., Robbins, J., Runglall, M., *et al.* (2016). Candidalysin is a fungal peptide toxin critical for mucosal infection. *Nature* *532*, 64-68.
- Nalleweg, N., Chiriack, M.T., Podstawa, E., Lehmann, C., Rau, T.T., Atreya, R., Krauss, E., Hundorfean, G., Fichtner-Feigl, S., Hartmann, A., *et al.* (2015). IL-9 and its receptor are predominantly involved in the pathogenesis of UC. *Gut* *64*, 743-755.
- Nieuwenhuizen, W.F., Pieters, R.H., Knippels, L.M., Jansen, M.C., and Koppelman, S.J. (2003). Is *Candida albicans* a trigger in the onset of coeliac disease? *Lancet* *361*, 2152-2154.
- Noble, S.M., Gianetti, B.A., and Witchley, J.N. (2017). *Candida albicans* cell-type switching and functional plasticity in the mammalian host. *Nat rev Microbiol* *15*, 96-108.
- Noverr, M.C., and Huffnagle, G.B. (2004). Does the microbiota regulate immune responses outside the gut? *Trends Microbiol* *12*, 562-568.
- Nowak, E.C., de Vries, V.C., Wasiuk, A., Ahonen, C., Bennett, K.A., Le Mercier, I., Ha, D.G., and Noelle, R.J. (2012). Tryptophan hydroxylase-1 regulates immune tolerance and inflammation. *J Exp Med* *209*, 2127-2135.
- Oberhuber, G., Granditsch, G., and Vogelsang, H. (1999). The histopathology of coeliac disease: time for a standardized report scheme for pathologists. *Eur J Gastroenterol Hepatol* *11*, 1185-1194.
- Pallotta, M.T., Orabona, C., Volpi, C., Vacca, C., Belladonna, M.L., Bianchi, R., Servillo, G., Brunacci, C., Calvitti, M., Biccato, S., *et al.* (2011). Indoleamine 2,3-dioxygenase is a signaling protein in long-term tolerance by dendritic cells. *Nat Immunol* *12*, 870-878.
- Papista, C., Gerakopoulos, V., Kourelis, A., Sounidaki, M., Kontana, A., Berthelot, L., Moura, I.C., Monteiro, R.C., and Yianguou, M. (2012). Gluten induces coeliac-like disease in sensitised mice involving IgA, CD71 and transglutaminase 2 interactions that are prevented by probiotics. *Lab Invest* *92*, 625-635.
- Pilette, C., Ouadrhiri, Y., Van Snick, J., Renauld, J.C., Staquet, P., Vaerman, J.P., and Sibille, Y. (2002). IL-9 inhibits oxidative burst and TNF-alpha release in lipopolysaccharide-stimulated human monocytes through TGF-beta. *J Immunol* *168*, 4103-4111.
- Reber, L.L., Sibilano, R., Mukai, K., and Galli, S.J. (2015). Potential effector and immunoregulatory functions of mast cells in mucosal immunity. *Mucosal Immunol* *8*, 444-463.
- Renauld, J.C., Goethals, A., Houssiau, F., Van Roost, E., and Van Snick, J. (1990). Cloning and expression of a cDNA for the human homolog of mouse T cell and mast cell growth factor P40. *Cytokine* *2*, 9-12.

- Rodrigues, C.P., Ferreira, A.C., Pinho, M.P., de Moraes, C.J., Bergami-Santos, P.C., and Barbuto, J.A. (2016). Tolerogenic IDO(+) Dendritic Cells Are Induced by PD-1-Expressing Mast Cells. *Front Immunol* 7, 9.
- Romani, L. (2011). Immunity to fungal infections. *Nat rev Immunol* 11, 275-288.
- Sasaki, K. (2012). Candida-associated gastric ulcer relapsing in a different position with a different appearance. *World J Gastroenterol* 18, 4450-4453.
- Schlapbach, C., Gehad, A., Yang, C., Watanabe, R., Guenova, E., Teague, J.E., Campbell, L., Yawalkar, N., Kupper, T.S., and Clark, R.A. (2014). Human TH9 cells are skin-tropic and have autocrine and paracrine proinflammatory capacity. *Sci Transl Med* 6, 219ra218.
- Schmitt, E., Klein, M., and Bopp, T. (2014). Th9 cells, new players in adaptive immunity. *Trends immunol* 35, 61-68.
- Schuurhof, A., Bont, L., Siezen, C.L., Hodemaekers, H., van Houwelingen, H.C., Kimman, T.G., Hoebee, B., Kimpen, J.L., and Janssen, R. (2010). Interleukin-9 polymorphism in infants with respiratory syncytial virus infection: an opposite effect in boys and girls. *Pediatr Pulmonol* 45, 608-613.
- Scott, B.B., and Jenkins, D. (1982). Gastro-oesophageal candidiasis. *Gut* 23, 137-139.
- Shelburne, C.P., Nakano, H., St John, A.L., Chan, C., McLachlan, J.B., Gunn, M.D., Staats, H.F., and Abraham, S.N. (2009). Mast cells augment adaptive immunity by orchestrating dendritic cell trafficking through infected tissues. *Cell Host Microbe* 6, 331-342.
- Shik, D., Tomar, S., Lee, J.B., Chen, C.Y., Smith, A., and Wang, Y.H. (2017). IL-9-producing cells in the development of IgE-mediated food allergy. *Semin Immunopathol* 39, 69-77.
- Speletas, M., Vyzantiadis, T.A., Kalala, F., Plastiras, D., Kokoviadou, K., Antoniadis, A., and Korantzis, I. (2008). Pneumonia caused by *Candida krusei* and *Candida glabrata* in a patient with chronic myeloid leukemia receiving imatinib mesylate treatment. *Med Mycol* 46, 259-263.
- Stecher, B. (2015). The Roles of Inflammation, Nutrient Availability and the Commensal Microbiota in Enteric Pathogen Infection. *Microbiol spectr* 3.
- Trevisan, E., Vita, F., Medic, N., Soranzo, M.R., Zabucchi, G., and Borelli, V. (2014). Mast cells kill *Candida albicans* in the extracellular environment but spare ingested fungi from death. *Inflammation* 37, 2174-2189.
- Underhill, D.M., and Pearlman, E. (2015). Immune Interactions with Pathogenic and Commensal Fungi: A Two-Way Street. *Immunity* 43, 845-858.
- Walker, W.A., Isselbacher, K.J., and Bloch, K.J. (1972). Intestinal uptake of macromolecules: effect of oral immunization. *Science* 177, 608-610.
- Weigmann, B., and Neurath, M.F. (2017). Th9 cells in inflammatory bowel diseases. *Semin Immunopathol* 39, 89-95.
- Wilhelm, C., Hirota, K., Stieglitz, B., Van Snick, J., Tolaini, M., Lahl, K., Sparwasser, T., Helmby, H., and Stockinger, B. (2011). An IL-9 fate reporter demonstrates the induction of an innate IL-9 response in lung inflammation. *Nat immunol* 12, 1071-1077.

Yamaguchi, N., Sugita, R., Miki, A., Takemura, N., Kawabata, J., Watanabe, J., and Sonoyama, K. (2006). Gastrointestinal *Candida* colonisation promotes sensitisation against food antigens by affecting the mucosal barrier in mice. *Gut* 55, 954-960.

Zelante, T., Iannitti, R.G., Cunha, C., De Luca, A., Giovannini, G., Pieraccini, G., Zecchi, R., D'Angelo, C., Massi-Benedetti, C., Fallarino, F., *et al.* (2013). Tryptophan catabolites from microbiota engage aryl hydrocarbon receptor and balance mucosal reactivity via interleukin-22. *Immunity* 39, 372-385.

## Figure legends

### Figure 1. The IL-9/IL-9R signaling pathway orchestrates innate and Th immunity to *C. albicans*.

C57BL/6, *Il9R*<sup>-/-</sup> and MC-deficient C57BL6-*Kit*<sup>W/W-v</sup> mice ( $n=6$ ) were infected intragastrically with *C. albicans* and evaluated for (A) IL-9 production, (B) *Il9R* gene expression in the stomach, (C) ILC2 and Th9 specific transcripts gene expression on Peyer's patches and purified CD4<sup>+</sup> T cells from mesenteric lymph nodes (MLN), (D) serum MCPT-1 levels, (E) Th-cell specific transcripts expression on CD4<sup>+</sup> T cells from MLN, (F) pro-inflammatory cytokines production in the stomach, (G) stomach and colon (in the insets) histopathology (periodic acid-Schiff staining) and (H) local fungal growth ( $\log_{10}$  CFU, mean  $\pm$  SD). (I) Fungal growth ( $\log_{10}$  CFU, mean  $\pm$  SD) and (J) inflammatory cytokines gene expression and production in the stomach of infected C57BL/6 mice ( $n=6$ ) treated intraperitoneally for a week with 10 mg/kg mAb neutralizing IL-9 or 10  $\mu$ g/kg rIL-9. Control (none) mice received isotype control antibody. Photographs were taken with a high-resolution microscope (Olympus DP71). Scale bars 200  $\mu$ m and 100  $\mu$ m. Cytokine levels were determined on stomach homogenates or serum by ELISA, gene expression by RT-PCR. Data are expressed as mean  $\pm$  SD. \* $P<0.05$ , \*\* $P<0.01$ , \*\*\* $P<0.001$ , \*\*\*\* $P<0.0001$ , knockout vs C57BL/6 mice and treated vs untreated mice. One- or two-way ANOVA, Bonferroni and Tukey's post test. Data represent pooled results or representative images from three experiments. Dpi, days post infection.

**Figure 2. The IL-9/IL-9R signaling pathway provides resistance to re-infection.** C57BL/6 and *Il9R*<sup>-/-</sup> mice ( $n=6$ ) were subjected to secondary intragastric infection with *C. albicans*. Mice were evaluated for (A) survival, (B) fungal growth ( $\log_{10}$  CFU, mean  $\pm$  SD), and (C) histopathology (periodic acid-Schiff staining) in different organs, (D) IL-9 levels, *Pu.1* and *Irf4* specific transcripts gene expression in the stomach, (E) Th-cell transcription factors expression and cytokines production. Photographs were taken with a high-resolution microscope (Olympus DP71). Scale bars 500  $\mu$ m and 100  $\mu$ m. Cytokines were determined on stomach homogenates by ELISA, gene expression by RT-PCR. Data are presented as mean  $\pm$  SD. \* $P<0.05$ , \*\* $P<0.01$ , \*\*\* $P<0.001$ , *Il9R*<sup>-/-</sup> vs C57BL/6 mice. Statistical analyses of the survival curves were performed using the Log-rank (Mantel-Cox) test. Unpaired T test or two-way ANOVA, Bonferroni post test. Data represent pooled results or representative images from three experiments. NS, not significant. Dpi, days post infection. Naïve, uninfected mice.

**Figure 3. The IL-9/IL-9R signaling pathway regulates mast cell activity in infection.** (A) Alcian blue/Safranin staining with relative mast cells (MC) number/mm<sup>2</sup> and (B) MC proteases gene expression in stomach sections of C57BL/6 and *Il9R*<sup>-/-</sup> mice infected intragastrically with *C. albicans*. (C) Percentage of degranulation in bone marrow-derived MC in the presence of IL-3 with (Connective Tissue-MC, CTMC) or without (Mucosal-MC, MMC) stem cell factor and stimulated with *C. albicans* yeasts, hyphae or IgE/Ag. (D) Mast cell morphometry (May-Grunwald Giemsa staining) and percentage of phagocytosis (upper line) and killing (lower line) of MMC and CTMC pulsed for 2 hours with viable *C. albicans* yeasts or hyphae. (E) MCPT-1 and (F) cytokine levels in culture supernatants of MMC and CTMC pulsed with the fungus for 5 hours with and without 10 ng/ml rIL-9. Photographs were taken with a high-resolution microscope (Olympus DP71). Scale bars 200  $\mu$ m and 50  $\mu$ m. Cytokines were determined on culture supernatants by ELISA, gene expression by RT-PCR. Data are presented as mean  $\pm$  SD. \* $P<0.05$ , \*\* $P<0.01$ , \*\*\* $P<0.001$ , \*\*\*\* $P<0.0001$ , *Il9R*<sup>-/-</sup> vs C57BL/6 mice and treated vs untreated (none) cells. One- or two-way ANOVA, Tukey's and Bonferroni post test. Data represent pooled results or representative images from two or three experiments. Dpi, days post infection.

**Figure 4. Mast cells regulate intestinal permeability and adaptive immunity in *C. albicans* infection.** In vivo intestinal permeability measured as (A) FITC-dextran levels in the serum, (B) colon *Occludin* gene expression and (C) kidney fungal growth ( $\log_{10}$  CFU, mean  $\pm$  SD) of C57BL/6, *Kit*<sup>W/W<sup>v</sup></sup> and *Il9R*<sup>-/-</sup> mice infected intragastrically with *C. albicans* and treated for 3 days with 10  $\mu$ g/kg rIL-9. *Kit*<sup>W/W<sup>v</sup></sup> mice were engrafted intravenously with wild-type bone marrow-cultured MC (BMMC). (D) Stomach histopathology (periodic acid-Schiff staining), (E) fungal growth ( $\log_{10}$  CFU, mean  $\pm$  SD), (F) inflammatory cytokines and (G) T helper specific transcription factors gene expression in C57BL/6 and *Kit*<sup>W/W<sup>v</sup></sup> mice ( $n=6$ ) subjected to primary and secondary intragastric infection. Photographs were taken with a high-resolution microscope (Olympus DP71). Scale bars 200  $\mu$ m and 50  $\mu$ m. Gene expression was determined by RT-PCR. Data are presented as mean  $\pm$  SD. \* $P<0.05$ , \*\* $P<0.01$ , \*\*\* $P<0.001$ , treated vs untreated mice and *Kit*<sup>W/W<sup>v</sup></sup> vs C57BL/6 mice. One- or two-way ANOVA, Tukey's or Bonferroni post test. Data represent pooled results or representative images from three experiments. Naïve, uninfected. None, untreated mice. Dpi, days post infection. R, 3 days after re-infection.

**Figure 5. IL-9 regulates indoleamine 2,3-dioxygenase (IDO)1 activity.** IDO1 expression by immunoblotting in the spleen (A) and in the colon (B) of C57BL/6 and *Il9R*<sup>-/-</sup> mice subjected to primary and secondary *C. albicans* infection. (C) TGF- $\beta$  production and (D) *Ptpn6* gene expression in the stomach of C57BL/6, *Il9R*<sup>-/-</sup> and *Kit*<sup>W/W<sup>v</sup></sup> mice infected as above. (E) *Tgfb*, *Ptpn6* and *Ido1* gene expression and (F) IDO1/STAT3 protein expression and phosphorylation on purified splenic dendritic cells pretreated with rIL-9 or  $\alpha$ IL-9 antibody for 1 hour before pulsing with the fungus for additional 5 hours. (G) *Tph1* gene expression in unstimulated MMC and CTMC and in the stomach of C57BL/6 and *Il9R*<sup>-/-</sup> mice infected and re-infected with the fungus. C57BL/6 and *Tph1*<sup>-/-</sup> mice ( $n=6$ ) were intragastrically infected with *C. albicans* and assessed for (H) stomach histopathology (periodic acid-Schiff staining), (I) local fungal growth ( $\log_{10}$  CFU, mean  $\pm$  SD) and (J) *Foxp3* gene expression and IL-10 production. Photographs were taken with a high-resolution microscope (Olympus DP71). Scale bars 200  $\mu$ m and 50  $\mu$ m. TGF- $\beta$  and IL-10 production was determined by ELISA and gene expression by RT-PCR. Data are expressed as mean  $\pm$  SD. \* $P<0.05$ , \*\* $P<0.01$ , \*\*\* $P<0.001$ , \*\*\*\* $P<0.001$ , knockout vs C57BL/6 mice and rIL-9-treated vs untreated (0) cells. Unpaired T test or two-way ANOVA, Tukey's or Bonferroni post test. Data represent pooled results or representative images from three experiments. Naïve, uninfected mice. Dpi, days post infection. R, 3 days after re-infection.

**Figure 6. IL-9 and MC affect gut microbial composition.** C57BL/6 and *Il9R*<sup>-/-</sup> mice were infected intragastrically with *C. albicans* and assessed for (A) relative abundance of major bacterial phyla and families and (B) taxonomic distribution of *Lactobacillus* species in the feces. (C) Detection of CD127<sup>+</sup>Ror $\gamma$ <sup>t</sup> cells on Peyer's patches by flow cytometry (numbers refer to percentages of positive cells), (D) *Ahr* expression and IL-22 production and (E) *Lcn2* expression in the stomach. (F) Lactobacillaceae distribution in the feces, (G) stomach fungal growth ( $\log_{10}$  CFU, mean  $\pm$  SD) and (H) histopathology (periodic acid-Schiff staining) in C57BL/6 and *Il9R*<sup>-/-</sup> mice infected as above 1 day after fecal microbiota transplantation (FMT). Photographs were taken with a high-resolution microscope (Olympus DP71). Scale bar 200  $\mu$ m. Bacterial abundance was evaluated by PCR, IL-22 production was determined by ELISA and gene expression by RT-PCR. Data are presented as mean  $\pm$  SD. \* $P<0.05$ , \*\* $P<0.01$ , \*\*\* $P<0.001$ , *Il9R*<sup>-/-</sup> vs C57BL/6 mice and FM-transplanted vs intact mice. Two-way ANOVA, Bonferroni post test. NS, not significant. Dpi, days post infection.

**Figure 7. IL-9/MMC are expanded in murine models of leaky gut and in human CD.** (A) IL-9 levels in the stomach, (B) Th9 specific transcripts gene expression, (C) MC proteases gene expression and (D) occludin expression in the gut of C57BL/6 and *Cftr*<sup>F508del</sup> mice ( $n=6$ ) infected intragastrically with *C. albicans*. (E) IL-9 levels in the small intestine, (F) Th9 specific transcripts gene expression, (G) MC proteases gene expression and

(H) occludin expression in BALB/c mice with gluten sensitivity. (I) IL-9 and IDO1 protein expression by immunofluorescence, detection of CD3<sup>+</sup>, CD117<sup>+</sup> and tryptase<sup>+</sup> cells by immunohistochemical staining in duodenal biopsies from patients with Marsh 1, Marsh 2, and Marsh 3 scores and controls (Ctrl). Photographs were taken with a high-resolution microscope (Olympus DP71). Scale bars 200  $\mu$ m and 100  $\mu$ m. IL-9 production was determined by ELISA and gene expression by RT-PCR. Data are presented as mean  $\pm$  SD. \*\*P<0.01, \*\*\*P<0.001, \*\*\*\*P<0.0001, *Cftr*<sup>F508del</sup> vs C57BL/6 and Gliadin- vs vehicle-treated mice. Unpaired T test or two-way ANOVA, Bonferroni post test. Data represent pooled results or representative images from three experiments. NS, not significant. Dpi, days post infection.

## Methods

**General experimental approaches.** Sample size was chosen empirically based on our previous experiences in the calculation of experimental variability; no statistical method was used to predetermine sample size and no samples, mice or data points were excluded from the reported analyses. Experimental groups were balanced in terms of animal age, sex and weight. No blinding was applied upon harvesting samples after the treatments.

**Mice.** Six to eight-weeks old C57BL/6 and five-weeks old BALB/c mice were purchased from Charles River (Calco, Italy). Homozygous mast cell (MC)-deficient C57BL/6-*Kit*<sup>W/W<sup>v</sup></sup>, *Tph1*<sup>-/-</sup>, *Il4*<sup>-/-</sup> and *Il17Ra*<sup>-/-</sup> mice were bred under specific pathogen-free conditions at the Animal Facility of Perugia University, Perugia, Italy. *Il9R*<sup>-/-</sup> and *Rag2*<sup>-/-</sup>*Il9R*<sup>-/-</sup> mice were kindly provided by Prof. Jean-Christophe Renauld (Ludwing Institute for Cancer Research, Brussels). CF mice homozygous for the Phe508del-*Cftr* allele, which had been backcrossed for 12 generations to the C57BL/6 strain or on the FVB/129 outbred background (*Cftr*<sup>tm1EUR</sup>, Phe508del, abbreviated *Cftr*<sup>F508del/F508del</sup>), were obtained from B. Scholte (Erasmus Medical Center). These mice were provided with a special food consisting of an equal mixture of SRM-A (Arie Blok, Woerden, The Netherlands) and Teklad 2019 (Harlan Laboratories, San Pietro al Natisone, Udine, Italy) and water acidified to pH 2.0 with HCl and containing 60 g/l PEG 3350, 1.46 g/l NaCl, 0.745 g/l KCl, 1.68 g/l NaHCO<sub>3</sub> and 5.68 g/l Na<sub>2</sub>SO<sub>4</sub>.

**Infections and treatments.** Gastrointestinal infection was performed by inoculating mice intragastrically (i.g.) with 10<sup>8</sup> *Candida albicans* cells in 200 µl saline using an 18-gauge 4-cm-long plastic catheter. Re-infection was performed by intragastric inoculation of 10<sup>8</sup> *Candida albicans* cells, 15 days after the primary infection. Quantification of fungal burden was performed at different days post-infection (dpi) by plating triplicate serial dilutions of homogenized organs in Sabouraud-dextrose agar. The results are expressed as colony-forming units (Log<sub>10</sub> CFU), per organ, ± SD. For vaginal infection, mice were injected subcutaneously with 100µl of 1g/ml β-estradiol 17-valerate (Sigma Chemical Co.) dissolved in sesame oil (Sigma-Aldrich) 48 h before vaginal infection. Estrogen administration continued weekly until completion of the study to maintain pseudoestrus. The estrogen-treated mice were inoculated intravaginally with 20 µl of phosphate-buffered saline (PBS) suspension of 5 x 10<sup>6</sup> viable *C. albicans* blastospores from early–stationary-phase cultures. CFUs are expressed as Log<sub>10</sub> CFU/100 ml of lavage fluid. Cytospin preparations of the lavage fluids were stained with May-Grünwald-Giemsa and observed with a BX51 microscope equipped with a high-resolution DP71 camera (Olympus). Murine monoclonal anti-IL-9 antibody (clone MM9C1; BioXcell), or control isotype IgG (clone C1.18.4; BioXcell) were administered intraperitoneally (i.p.) at dose of 10 mg/kg for a week starting the day of the infection (from 344,33±68,07 pg/ml to undetectable levels in the stomach, untreated vs treated mice at 3 dpi). Recombinant (r)IL-9 (R&D System) was administered i.p. at the dose of 10 µg/kg (Blankenhaus et al., 2014). Selective engraftment of MC in MC-deficient C57BL/6-*Kit*<sup>W/W<sup>v</sup></sup> mice was performed injecting into each mouse, via the tail vein, 5x10<sup>6</sup> bone marrow cells derived from 6-week-old female C57BL/6 mice cultured in WEHI-3–

conditioned medium (ATCC number TIB-68), as a source of IL-3, for 4–5 weeks. The recipients were used for experiments 4 weeks later.

**Histological, immunofluorescence and immunohistochemical staining and immunoblotting analysis.** For histology, paraffin-embedded tissue sections (3–4 mm) were stained with Periodic acid-Schiff (Dudeck et al.) or, for colons, with Hematoxylin and Eosin. For mast cells (MCs) count, stomach sections were stained with Toluidine Blue and MCs were counted in images. Tissue areas were calculated using NIH Image J software. For MC differentiation, stomach sections were stained with Alcian blue (AB) and Safranin (S), dyes commonly used to differentially stain CTMC, that do not stain with Alcian blue but stain with safranin (AB<sup>-</sup>S<sup>+</sup>) and MMC that show the reverse staining pattern (AB<sup>+</sup>S<sup>-</sup>) (Feyerabend et al., 2005). For immunofluorescence, intestinal sections from mice were incubated at 4°C with anti-Occludin (Invitrogen) antibody. Duodenal biopsies sections from celiac patients or controls were incubated at 4°C with anti-IL-9 (BioLegend) or anti-IDO1 (Santa Cruz) antibodies followed by secondary FITC or TRITC (all from Sigma Aldrich) antibodies respectively. 4'-6-Diamino-2-phenylindole (DAPI) was used to detect nuclei. Immunohistochemistry was performed on 4 µm sections using the monoclonal antibodies CD3 (Leica, clone LN10), CD117 (Dako, clone c-kit) and mast cell tryptase (Leica, clone 10D11). The primary antibody was detected using a biotin-free polymeric-horseradish peroxidase (HRP)-linker antibody conjugate system (Bond Polymer Refine Detection, Leica BioSystems) with heat-induced epitope retrieval, using the Bond III automated immunostainer (Leica BioSystems). Photographs were taken using a high-resolution Olympus DP71 microscope. For immunoblotting, organs or cells were lysed in RIPA buffer. The lysate was separated in SDS-PAGE and transferred to a nitrocellulose membrane. Blot of lysates were incubated with the following antibodies: anti-mouse polyclonal IDO1 (Millipore), p-IDO (specifically recognizing the phosphorylated ITIM2 motif in IDO1), monoclonal STAT3 (Cell Signaling, clone 124H6) and polyclonal phospho (p)-STAT3 (Cell Signaling). Normalization was performed by probing the membrane with mouse-monoclonal anti-β-tubulin, anti-Gapdh and anti-β-actin antibody (all from Sigma-Aldrich). Images were acquired with LiteAblotPlus chemiluminescence substrate (Euroclone S.p.A.), using ChemiDoc™ XRS+Imaging system (Bio-Rad Laboratories) and quantification was obtained by densitometry image analysis using Image Lab 5.1 software (Bio-Rad).

**Cell purification and culture.** CD4<sup>+</sup> T cells were purified after incubation of mesenteric lymph nodes with Type IV Collagenase and DNase followed by magnetic separation with CD4 microbeads (Miltenyi Biotec). Lineage negative (Lin<sup>-</sup>) cells were isolated from Peyer's patches (PP) digested with Type IV Collagenase (Sigma-Aldrich) by magnetic depletion with Lineage Positive cells kit (Miltenyi Biotec). Mouse bone marrow mast cells (BMMC) were obtained by culturing bone marrow from 4-wk-old C57BL/6 mice for 4 weeks in enriched medium (RPMI 1640 containing 2 mM L-glutamine, Non-Essential Aminoacids, 100 IU/ml Pen-strep, 1 mM sodium pyruvate, 20 mM Hepes, 50 mM 2-Mercaptoethanol and 20% FCS) supplemented with 20 ng/ml murine rIL-3 alone or with 100 ng/ml stem cell factor (SCF), to obtain MC considered to be the tissue culture

equivalent of mucosal MC (MMC) or connective tissue (CTMC) (Godfraind et al., 1998), respectively. MC, either alone or IgE-sensitized, were stimulated with 10 ng/ml rIL-9 for 1 hour before 5 hours pulsing with *C. albicans* yeasts or hyphae (at cell:fungi ratio 1:1) for the assessment of degranulation percentage. MC pre-stimulated as above, were also evaluated for cytokine and specific protease production in the supernatants of cells after 4 hours culture with the fungus (at cell:fungi ratio 1:1) and for phagocytosis and killing of both *C. albicans* morphotypes after 2 hours pulsing (at cell:fungi ratio 1:1 or 10:1 respectively). For IgE sensitization, MC were sensitized in medium without IL-3 overnight with 1 µg/mL of DNP-specific IgE and washed twice with Tyrode's buffer (10 mM HEPES buffer (pH 7.4), 130 mM NaCl, 5 mM KCl, 1.4 mM CaCl<sub>2</sub>, 1 mM MgCl<sub>2</sub>, 5.6 mM glucose and 0.1% BSA). MC were then challenged with 1 µg/mL of DNP-HSA in Tyrode's buffer/0.05% BSA.

**Intestinal permeability.** Intestinal permeability was measured in C57BL/6, C57BL/6-*Kit*<sup>W/W<sup>v</sup></sup>, either intact or engrafted intravenously with wild-type BMMC and *IL9R*<sup>-/-</sup> mice each naïve or treated for 3 days with 10 µg/kg rIL-9 and infected intragastrically with *C. albicans*. At the time of sacrifice, 3 days after infection, mice were fasted for 4 h orally with the exception of drinking water prior to the administration of 40mg/100g mouse weight of FITC-dextran (4kDa; Sigma-Aldrich) as described (Chen et al., 2008). Serum was collected retro-orbitally 4 h later and diluted 1:3 in PBS. The amount of fluorescence at 488 nm for emission and absorption at 525 nm, was read on the Infinite 200 plate reader (Tecan) using the manufacturer's I-control version 1.3 software.

**Bacterial DNA extraction and quantitative PCR for microbiota analysis.** Bacterial DNA from feces of C57BL/6 and *IL9R*<sup>-/-</sup> mice was extracted using a QIAamp DNA Stool Mini Kit (Qiagen). Bacteria species-specific PCR was carried out with primers listed in Supplementary Table 1 targeted on the 16S rRNA (Cha et al., 2010; Haarman and Knol, 2006; Mikelsaar et al., 2010) using BioRad MyCycler (BioRad) and Platinum Taq DNA Polymerase (Invitrogen). The amplification program was 94°C for 5 min, followed by 35 cycles of 94°C for 30 s, 30 s at the appropriate annealing temperature and 72°C for 30 s. A cycle of 72°C for 10 min concluded the program. Amplification products were detected by agarose gel electrophoresis on 1,8% agarose gel, Gel Red™ (Biotium) staining and UV transillumination. Relative bacterial abundances from mean copy numbers for each bacterium were compared among all three groups of infected mice. Bacterial concentrations were calculated as percentages relative to the total bacterial 16S rRNA gene copy number, normalized to the control mouse group, and expressed as mean fold changes ± SD.

**Flow cytometry analysis.** Flow cytometry analysis was performed on enriched Lin<sup>-</sup> cells magnetically depleted from PP of C57BL/6 and *IL9R*<sup>-/-</sup> mice infected intragastrically with *C. albicans* and evaluated at different dpi. Cells were stained with a combination of the following fluorescence-conjugated mAbs (all from Miltenyi Biotec): PE-conjugated anti-CD127 (A7R 34); APC-conjugated anti-Rory (t) (REA278). For intracellular staining, cells were permeabilized with the CytoFix/CytoPerm kit (BD Biosciences) for intra-cytoplasmic

detection of Rory (t). Flow cytometry was done at 4°C on cells first exposed to Fc receptor mAb (2.4G2). Cells were analysed with a BD LSRFortessa flow cytometer equipped with BD FACSDiva 7.0 software.

**Fecal microbiota transplantation.** Six-week-old C57BL/6 and *Il9R<sup>-/-</sup>* recipient mice were treated with a “cocktail” of antibiotics containing vancomycin (500 mg/l) and neomycin (1g/l) in drinking water for a week followed by intraperitoneal injection of clindamycin (10 mg/kg) for two consecutive days before fecal transplantation (Murakami et al., 2016). Freshly harvested donor feces (0.8-1.0 mg feces/g BW/day) were resuspended in PBS, mixed with vortex for 10 min and administered by gavaging to recipient mice for 5 days, once a day. After transplantation, mice were infected intragastrically with 10<sup>8</sup> *Candida albicans* and sacrificed 3 days after infection.

**Murine model of celiac disease.** Three-generation gluten-free diet (Mucedola) (Papista et al., 2012), 5-week-old BALB/c male and female purchased from Charles River, were challenged via gavage with gliadin (10 mg/mice in 100 µl saline) 3 times week, for 4 weeks. At the end of the last daily treatment, mice were anesthetized with Avertine (Sigma Aldrich) and then killed; the small intestines were collected and stored for all described techniques. These studies and procedures were approved by the local Ethics Committee for Animal Welfare (IACUC No 583) and conformed to the European Community regulations for animal use in research (2010/63 UE).

**Antifungal effector activity.** Monolayers of plastic-adherent macrophages (Mφ) were obtained, after 2 hours plastic adherence, from splenic populations of C57BL/6 or *Il9R<sup>-/-</sup>* mice either naïve or intragastrically infected with *C. albicans*. Cells were pretreated for 1h with 10 ng/mL rIL-9 before pulsing with *Candida* yeast (1:10 cell/fungus ratio). For oxidant production, Mφ were evaluated for oxidation of dihydrorhodamine 123 (DHR, Molecular Probes) measured by fluorimetry with the multifunctional microplate reader Tecan Infinite 200 (Tecan) at different time points. The percentage of CFU inhibition (means±SD), referred to as candidacidal activity, was determined as described previously (Bellocchio et al., 2004).

**ELISA and real-time PCR.** The levels of cytokines in stomach and colon homogenates, sera and culture supernatants were determined by specific ELISAs (R&D System) following manufacturer’s instructions. Real-time RT-PCR was performed using CFX96 Touch Real-Time PCR Detection System and SYBR Green chemistry (BioRad). Cells were lysed and total RNA was reverse transcribed with cDNA Synthesis Kit (BioRad), according to the manufacturer’s instructions. The PCR primers were as listed in Supplementary Table 1. Amplification efficiencies were validated and normalized against *Gapdh*. The thermal profile for SYBR Green real-time PCR was at 95°C for 3 min, followed by 40 cycles of denaturation for 30 s at 95°C and an annealing/extension step of 30 sec at 60°C. Each data point was examined for integrity by analysis of the amplification plot. The mRNA-normalized data were expressed as relative gene mRNA in treated compared to untreated experimental groups or cells.

**Statistical analysis.** GraphPad Prism software 6.01 (GraphPad Software) was used for analysis. Data are expressed as means  $\pm$ SD. Horizontal bars indicate the means. Statistical significance was calculated by One- or two-way ANOVA (Tukey's or Bonferroni's post hoc test) for multiple comparisons and by a two-tailed Student's t-test for single comparisons. Statistical analysis of the survival curves was performed using the Log-rank (Mantel-Cox) test. The distribution of levels tested by the Kolmogorov–Smirnov normality test turned out to be non-significant. Fluorescence intensity was measured by using the ImageJ software. The variance was similar in the groups being compared. We considered all P values 0.05 to be significant. The in vivo groups consisted of six mice/group. The data reported are either representative of at least three experiments (histology, immunofluorescence and western blotting) or pooled otherwise.

**Ethics Statement.** Murine experiments were performed according to the Italian Approved Animal Welfare Authorization 360/2015-PR and Legislative decree 26/2014 regarding the animal license obtained by the Italian Ministry of Health lasting for five years (2015-2020). All efforts were made to minimize suffering. Male and female mice were used in all studies. For human duodenal biopsies, no individual patient identification was involved and no study-driven clinical intervention was performed; therefore, no ethical approval was necessary.

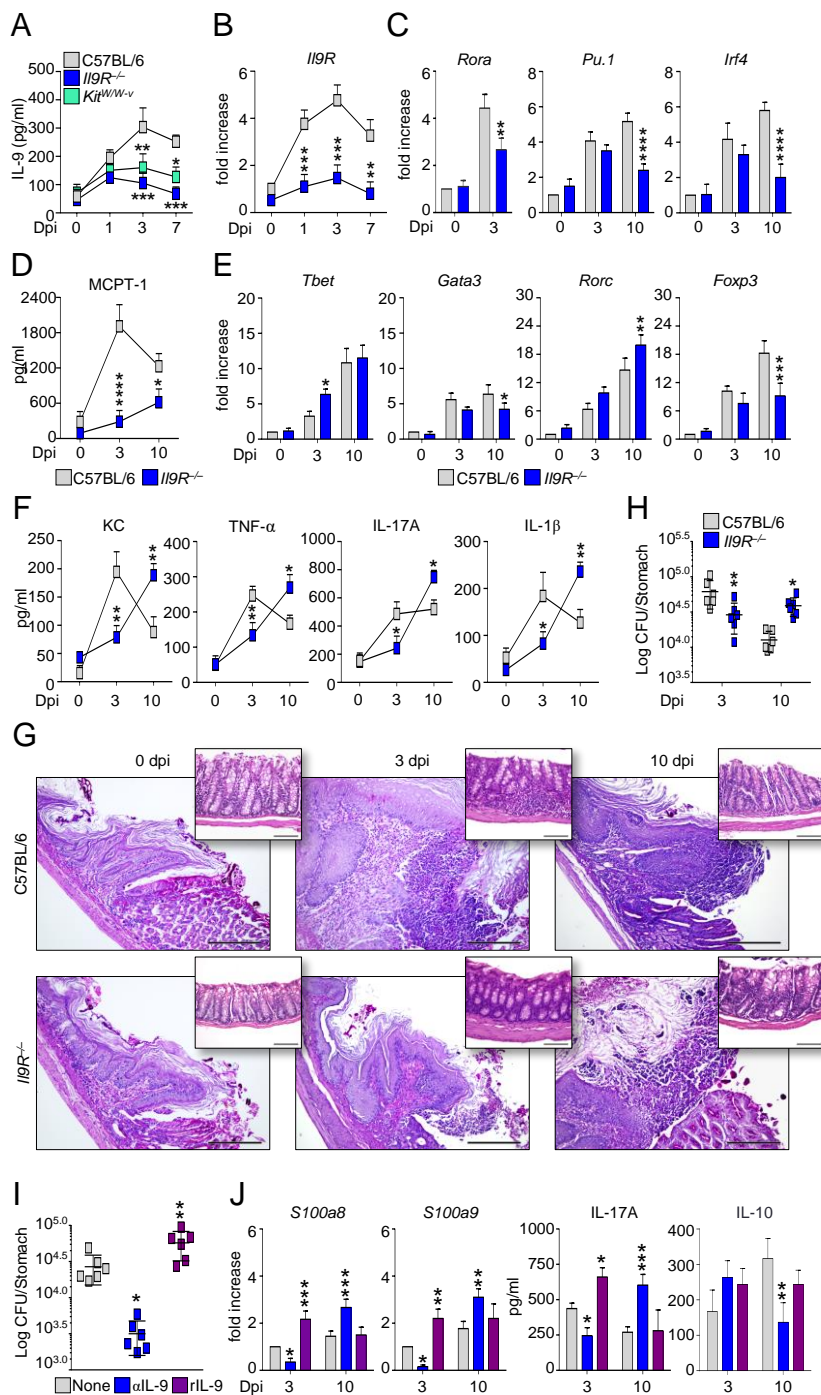
## References

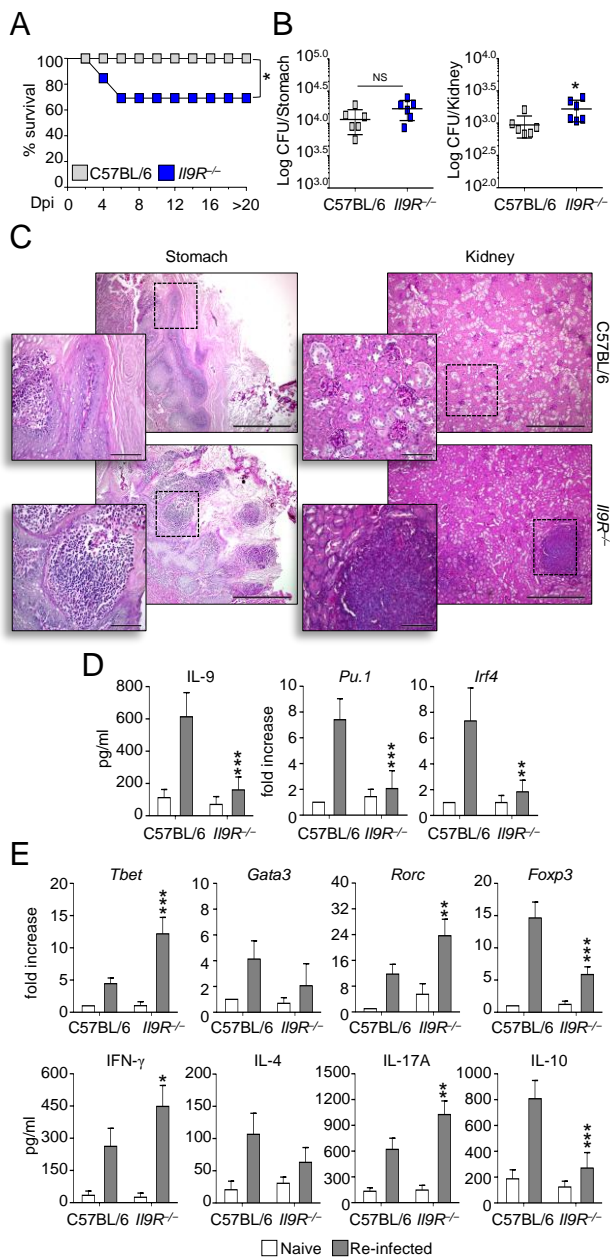
- Bellocchio, S., Moretti, S., Perruccio, K., Fallarino, F., Bozza, S., Montagnoli, C., Mosci, P., Lipford, G.B., Pizzurra, L., and Romani, L. (2004). TLRs govern neutrophil activity in aspergillosis. *J Immunol* *173*, 7406-7415.
- Blankenhaus, B., Reitz, M., Brenz, Y., Eschbach, M.L., Hartmann, W., Haben, I., Sparwasser, T., Huehn, J., Kuhl, A., Feyerabend, T.B., *et al.* (2014). Foxp3(+) regulatory T cells delay expulsion of intestinal nematodes by suppression of IL-9-driven mast cell activation in BALB/c but not in C57BL/6 mice. *PLoS Path* *10*, e1003913.
- Cha, C.H., An, H.K., and Kim, J.U. (2010). [Detection of vancomycin-resistant enterococci using multiplex real-time PCR assay and melting curve analysis]. *Korean J Lab Med* *30*, 138-146.
- Chen, G.Y., Shaw, M.H., Redondo, G., and Nunez, G. (2008). The innate immune receptor Nod1 protects the intestine from inflammation-induced tumorigenesis. *Cancer Res* *68*, 10060-10067.
- Dudeck, J., Ghouse, S.M., Lehmann, C.H., Hoppe, A., Schubert, N., Nedospasov, S.A., Dudziak, D., and Dudeck, A. (2015). Mast-Cell-Derived TNF Amplifies CD8(+) Dendritic Cell Functionality and CD8(+) T Cell Priming. *Cell Rep* *13*, 399-411.
- Feyerabend, T.B., Hausser, H., Tietz, A., Blum, C., Hellman, L., Straus, A.H., Takahashi, H.K., Morgan, E.S., Dvorak, A.M., Fehling, H.J., *et al.* (2005). Loss of histochemical identity in mast cells lacking carboxypeptidase A. *Mol Cell Biol* *25*, 6199-6210.
- Godfraind, C., Louahed, J., Faulkner, H., Vink, A., Warnier, G., Grecis, R., and Renaud, J.C. (1998). Intraepithelial infiltration by mast cells with both connective tissue-type and mucosal-type characteristics in gut, trachea, and kidneys of IL-9 transgenic mice. *J Immunol* *160*, 3989-3996.
- Haarman, M., and Knol, J. (2006). Quantitative real-time PCR analysis of fecal *Lactobacillus* species in infants receiving a prebiotic infant formula. *Appl Environ Microbiol* *72*, 2359-2365.
- Mikelsaar, M., Stsepetova, J., Hutt, P., Kolk, H., Sepp, E., Loivukene, K., Zilmer, K., and Zilmer, M. (2010). Intestinal *Lactobacillus* sp. is associated with some cellular and metabolic characteristics of blood in elderly people. *Anaerobe* *16*, 240-246.
- Murakami, M., Tognini, P., Liu, Y., Eckel-Mahan, K.L., Baldi, P., and Sassone-Corsi, P. (2016). Gut microbiota directs PPARgamma-driven reprogramming of the liver circadian clock by nutritional challenge. *EMBO reports* *17*, 1292-1303.
- Papista, C., Gerakopoulos, V., Kourelis, A., Sounidaki, M., Kontana, A., Berthelot, L., Moura, I.C., Monteiro, R.C., and Yiangou, M. (2012). Gluten induces coeliac-like disease in sensitised mice involving IgA, CD71 and transglutaminase 2 interactions that are prevented by probiotics. *Lab Invest* *92*, 625-635.

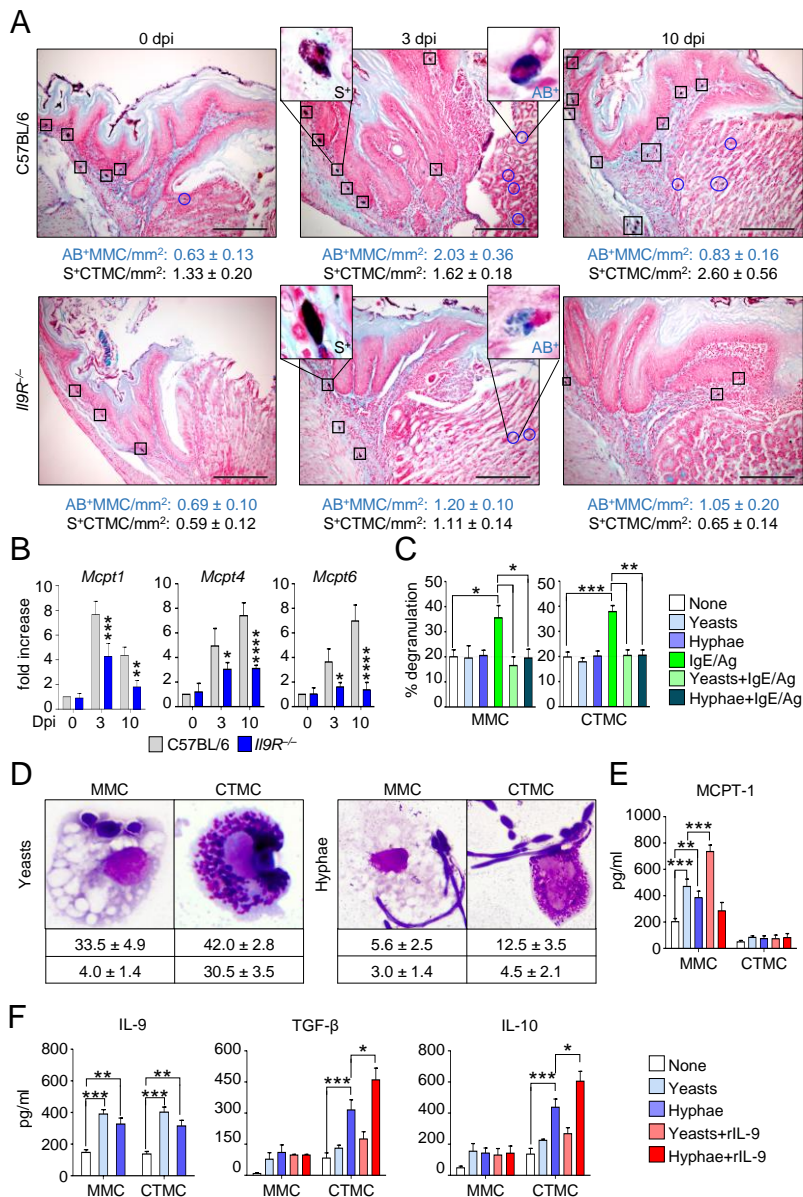
**Supplementary Table 1. List PCR primers used in this study**

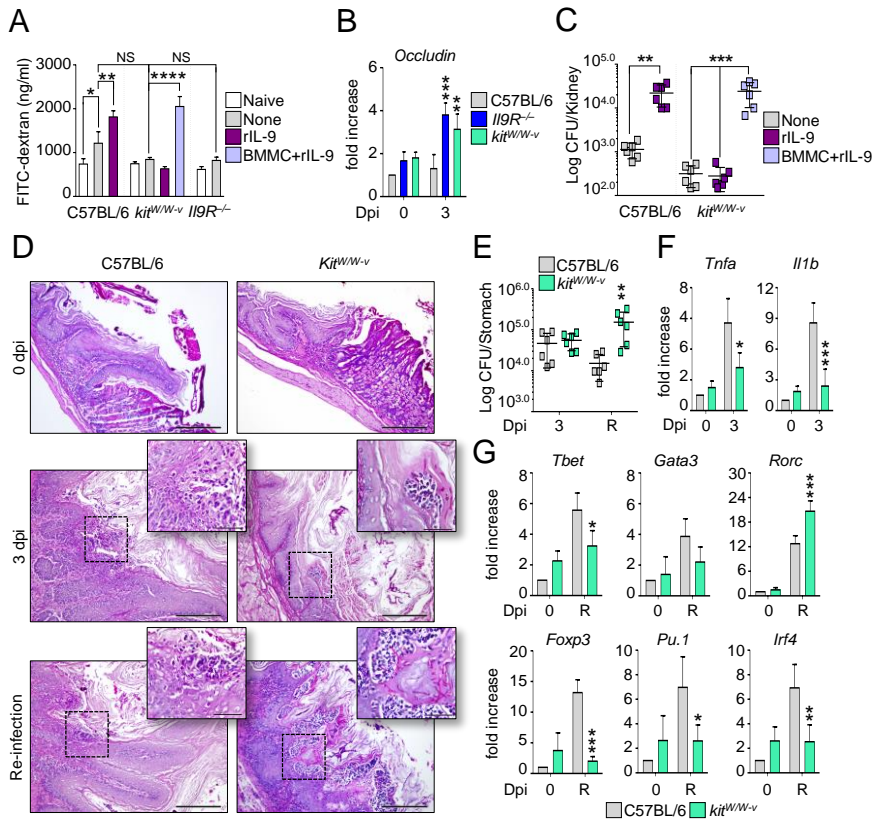
Gene name	Primer sequence
<i>Il9R</i>	Forward, 5'- ATGGGACAGGAACAGGTCAG -3'
	Reverse, 5'- TCCAGGGCAAGATTGATACC -3'
<i>Rora</i>	Forward, 5'- GGTCGGATGTCCAAGAAGCAGAG -3'
	Reverse, 5'- GATGTTGTAGGTGGGCGTCAGC -3'
<i>Gata3</i>	Forward, 5'- TCTGGAGGAGGAACGCTAATG -3'
	Reverse, 5'- GGCTGGAGTGGCTGAAGG -3'
<i>Pu.1</i>	Forward, 5'- GGCCTAACCCCTCCACCTA -3'
	Reverse, 5'- TCTGGCTGGTGAAGTCCTCT -3'
<i>Irf4</i>	Forward, 5'- GACCAGTCACACCCAGAAATCC -3'
	Reverse, 5'- TGGGGCACAAGCATAAAAGGTT -3'
<i>Tbet</i>	Forward, 5'- GGACGATCATCTGGGTACATTGT -3'
	Reverse, 5'- GCCAGGGAACCGTTATATG -3'
<i>Rorc</i>	Forward, 5'- ACAACAGCAGCAAGTGATGG -3'
	Reverse, 5'- CCTGGATTTATCCCTGCTGA -3'
<i>Foxp3</i>	Forward, 5'- CCCAGGAAAGACAGCAACCTTTT -3'
	Reverse, 5'- TTCTCACAACCAGGCCACTTG -3'
<i>S100a8</i>	Forward, 5'- TCGTGACAATGCCGTCTGAACTG -3'
	Reverse, 5'- TGCTACTCCTTGTGGCTGTCTTTG -3'
<i>S100a9</i>	Forward, 5'- CGCAGCATAACCACCATCATC -3'
	Reverse, 5'- GCCATCAGCATCATACTCC -3'
<i>Ido1</i>	Forward, 5'- CCCACACTGAGCACGGACGG -3'
	Reverse, 5'- GCCCTTGTCGCAGTCCCCAC -3'
<i>Ahr</i>	Forward, 5'- CACTGGATGCGTAGGTTCTTGG -3'
	Reverse, 5'- TCTTCATCCGTCAGTGGTCTC -3'
<i>Lcn2</i>	Forward, 5'- GGTGGTGAGTGTGGCTGAC -3'
	Reverse, 5'- CCTTGGTATGGTGGCTGGTG -3'
<i>Tnfa</i>	Forward, 5'- CGAGTGACAAGCCTGTAGCC -3'
	Reverse, 5'- AAGAGAACCTGGGAGTAGACAAG -3'
<i>Il1b</i>	Forward, 5'- TGACGGACCCCAAAGATGAAGG -3'
	Reverse, 5'- CCACGGGAAAGACACAGGTAGC -3'
<i>Occludin</i>	Forward, 5'- GTTGATCCCCAGGAGGCTAT -3'
	Reverse, 5'- CCATCTTTCTTCGGGTTTTTC -3'
<i>Mcpt1</i>	Forward, 5'- TCGAAAAACAAATCATTACAAA -3'
	Reverse, 5'- GACCAGGCAAGGGAATTACA -3'
<i>Mcpt4</i>	Forward, 5'- AAAACAAATCGTTCACCCAAA -3'
	Reverse, 5'- GTCAGAAGGACGAGGCAGAG -3'
<i>Mcpt6</i>	Forward, 5'- TTCTGCGGAGGTTCTCTCAT-3'
	Reverse, 5'- TACTGCTCACGAAGCTGCAC -3'
<i>Tph1</i>	Forward, 5'- GTCCCGGAAATCAAAGCAAAGA-3'
	Reverse, 5'- GGGCGAGTCCACCGAGAGG -3'
<i>Ptpn6</i>	Forward, 5'- CAGCTGCTAGGTCCAGATGAGA-3'
	Reverse, 5'- CAGCTCAGGTAAGTGGTAGTGC-3'
<i>Tgfb1</i>	Forward, 5'- CACAGAGAAGAAGTCTGTG-3'
	Reverse, 5'- AGGAGCGCACAATCATGTTG-3'

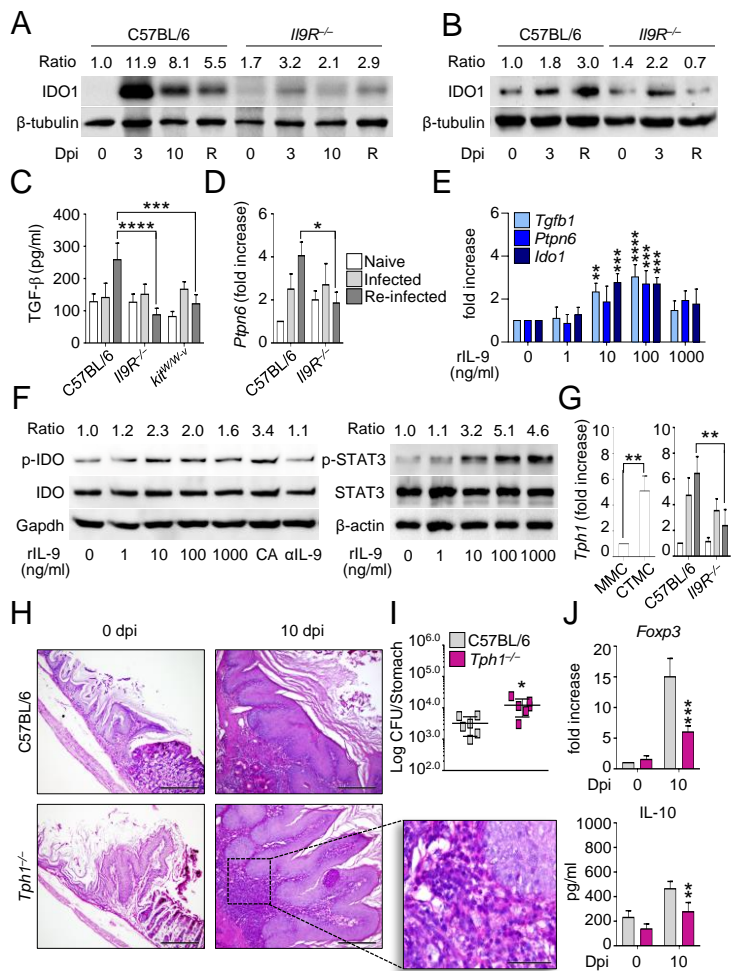
Eubacteria (all bacteria)	Forward, 5'- ACTCCTACGGGAGGCAGCAG -3'
	Reverse, 5'- ATTACCGCGGCTGCTGG -3'
Bacteroidetes	Forward, 5'- GGARCATGTGGTTTAATTCGATGAT -3'
	Reverse, 5'- AGCTGACGACAACCATGCAG -3'
Firmicutes	Forward, 5'- GGAGYATGTGGTTTAATTCGAAGCA -3'
	Reverse, 5'- AGCTGACGACAACCATGCAC -3'
Proteobacteria	Forward, 5'- CCGCAAGGTTAAACTCAAAGGAA -3'
	Reverse, 5'- CAGACATGTCAAGGGTAGGTAAGG -3'
Others	Forward, 5'- GGCCGTCGTCAGCTCGTGTCG -3'
	Reverse, 5'- CGTTACCGGGCAGTCCTACCAGA -3'
<i>Lactobacillus</i> <i>spp.</i>	Forward, 5'- TGGATGCCTTGGCACTAGGA -3'
	Reverse, 5'- AAATCTCCGGATCAAAGCTTACTTAT -3'
<i>Prevotellaceae</i>	Forward, 5'- CCGAAAGGCAGACTAATACCC -3'
	Reverse, 5'- TACCCCGCCAACAAGCTAATCAGA -3'
<i>Enterobacteriaceae</i>	Forward, 5'- CAGGTCGTCACGGTAACAAG -3'
	Reverse, 5'- GTGGTTCAGTTTCAGCATGTAC -3'
<i>Clostridiaceae</i>	Forward, 5'- AGCGTTGTCCGGATTTACTG -3'
	Reverse, 5'- CGCTTACCTCTCCGACACTC -3'
<i>L. acidophilus</i>	Forward, 5'- GAAAGAGCCCAAACCAAGTGATT -3'
	Reverse, 5'- CTCCCAGATAATTCAACTATCGCTTA -3'
<i>L. johnsonii</i>	Forward, 5'- GTGAGAGCCCCGTAC -3'
	Forward, 5'- CTACCACGCATATAATATA -3'
<i>L. murinus</i>	Forward, 5'- TGAAGAAGGTCTTCGGATCG -3'
	Reverse, 5'- TAAATCCGGATAACGCTTGC -3'
<i>L. reuteri</i>	Forward, 5'- TGAAGAAGGTCTTCGGATCG -3'
	Reverse, 5'- TAAATCCGGATAACGCTTGC -3'

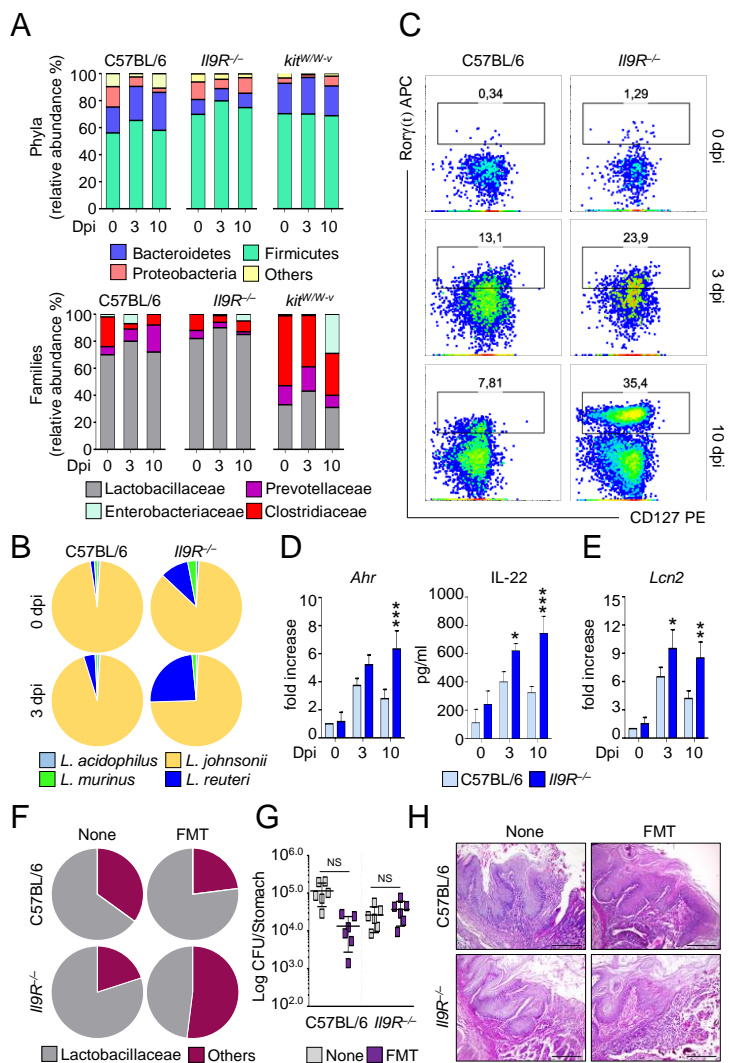


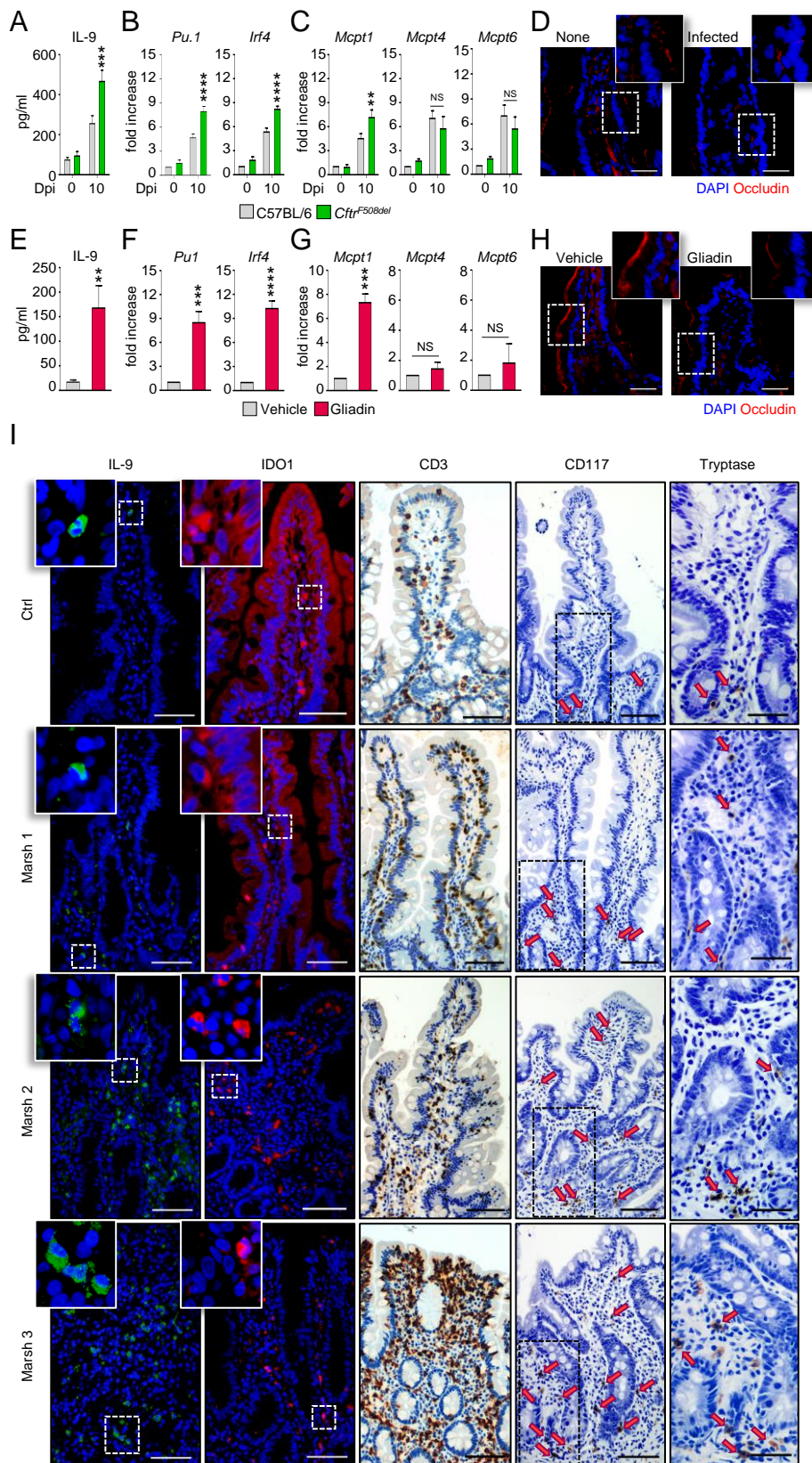












## Supplementary information

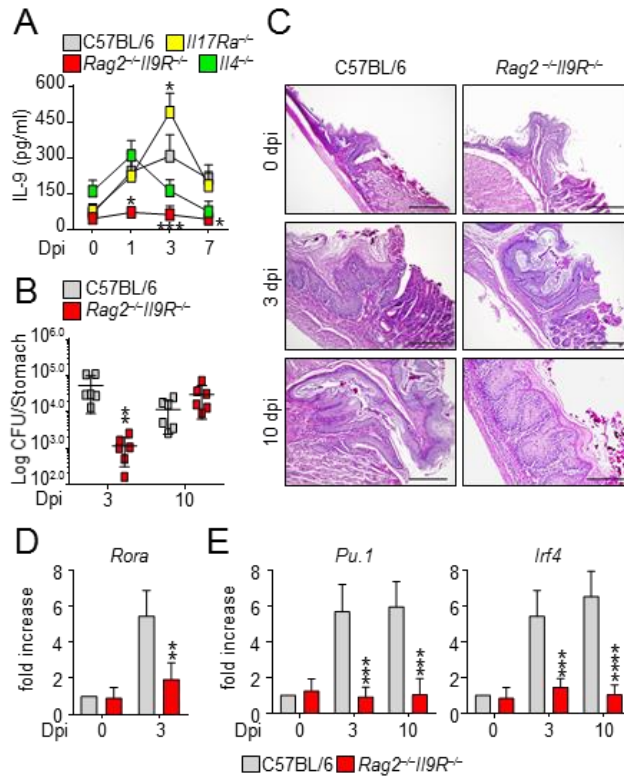


**Figure S1, related to Figure 1. The IL-9/IL-9R signaling pathway orchestrates innate and adaptive immunity to *C. albicans*.** (A) Time-course of IL-9 production in C57BL/6, *Il17Ra*<sup>-/-</sup>, *Rag2*<sup>-/-</sup>*Il9R*<sup>-/-</sup> and *Il4*<sup>-/-</sup> mice ( $n=6$ ) intragastrically infected with *C. albicans*. (B) Stomach fungal growth ( $\log_{10}$  CFU, mean  $\pm$  SD), (C) stomach histopathology (periodic acid-Schiff staining), (D and E) ILC2 and Th9 specific transcripts gene expression on Peyer's patches and purified CD4<sup>+</sup> T cells from mesenteric lymph nodes respectively of infected mice. Photographs were taken with a high-resolution microscope (Olympus DP71). Scale bar 200  $\mu$ m. IL-9 levels were determined on stomach homogenates by ELISA, gene expression by RT-PCR. Data are expressed as mean  $\pm$  SD. \* $P<0.05$ , \*\* $P<0.01$ , \*\*\* $P<0.001$ , \*\*\*\* $P<0.0001$ , knockout vs C57BL/6 mice. Two-way ANOVA, Bonferroni and Tukey's post test. Data represent pooled results or representative images from three experiments. Dpi, days post infection.

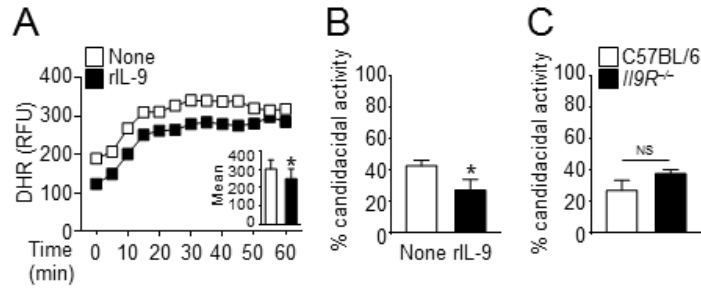


**Figure S2, related to Figure 3. IL-9 impacts on effector phagocytic activity.** (A) Oxidant production (by DHR at 60 min) and (B) candidacidal activity assessed in peritoneal polymorphonuclear cells pre-stimulated for 1 hour with 10 ng/ml of rIL-9 before pulsing with *C. albicans*. (C) Candidacidal activity assessed on splenic macrophages from C57BL/6 and *IL9R<sup>-/-</sup>* mice infected intragastrically with *C. albicans*. Shown in the insets of panel A the relative slope with error bars representing the mean  $\pm$  SD. Data are expressed as mean  $\pm$  SD. \* $P < 0.05$ , rIL-9-treated vs untreated mice and *IL9R<sup>-/-</sup>* vs C57BL/6 mice. Unpaired T test. Data represent pooled results three experiments. NS, not significant.

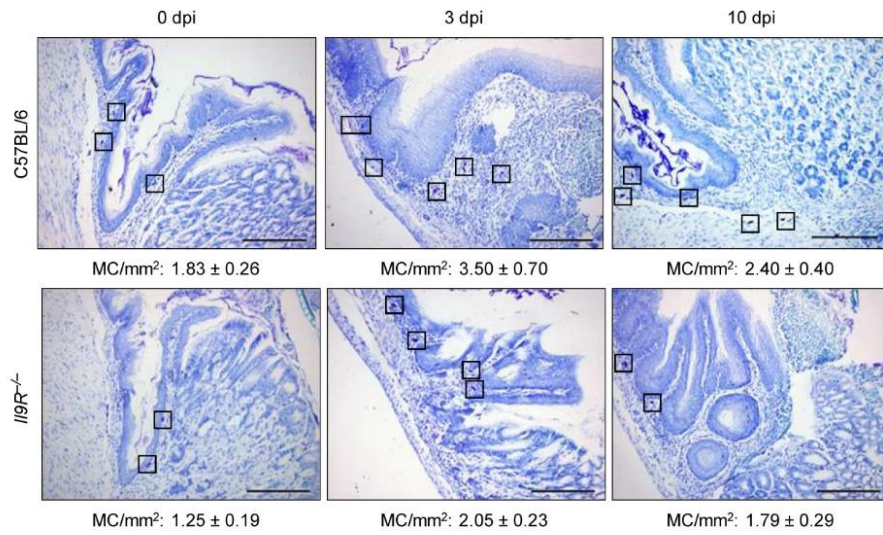


**Figure S3, related to Figure 3. Mast cells failed to expand in the stomach of infected *Il9R*<sup>-/-</sup> mice.** Toluidine blue staining with relative mast cells (MC) number/mm<sup>2</sup> in stomach sections of C57BL/6 and *Il9R*<sup>-/-</sup> mice (*n*=6) infected intragastrically with *C. albicans*. Data are representative images from three experiments. Dpi = days post infection.

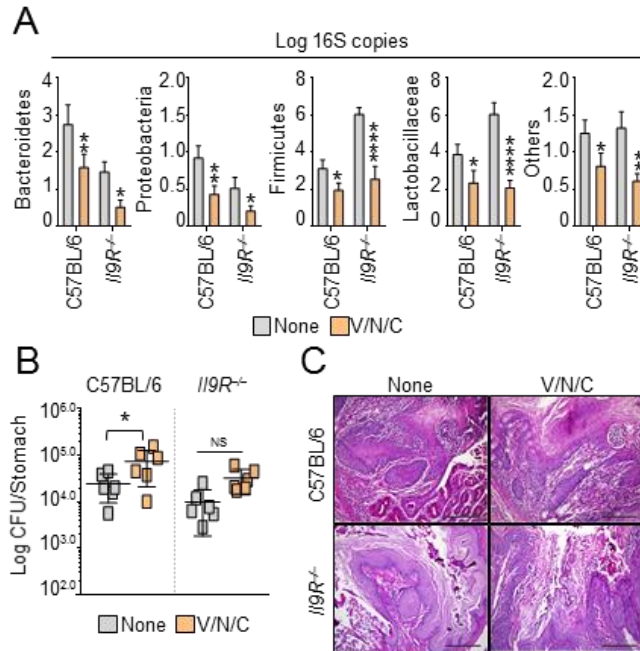


**Figure S4, related to Figure 6. Contribution of local microbiota to *C. albicans* susceptibility.** C57BL/6 and I19R<sup>-/-</sup> mice ( $n=6$ ) were treated with a cocktail of antibiotics [Vancomycin (V), Neomycin (N) and Clindamycin (C)] before intragastric infection with *C. albicans*. Mice were assessed 3 days after infection for (A) relative abundance of major bacterial phyla and taxa in the feces, (B) stomach fungal growth ( $\log_{10}$  CFU, mean  $\pm$  SD) and (C) stomach histopathology (periodic acid-Schiff staining). Photographs were taken with a high-resolution microscope (Olympus DP71). Scale bar 200  $\mu$ m. Bacterial abundance was evaluated by PCR. Data are expressed as mean  $\pm$  SD. \* $P<0.05$ , \*\* $P<0.01$ , \*\*\* $P<0.0001$ , Antibiotics-treated vs untreated mice. One-way and two-way ANOVA, Bonferroni and Tukey's post test. Data represent pooled results or representative images from three experiments. NS, not significant.

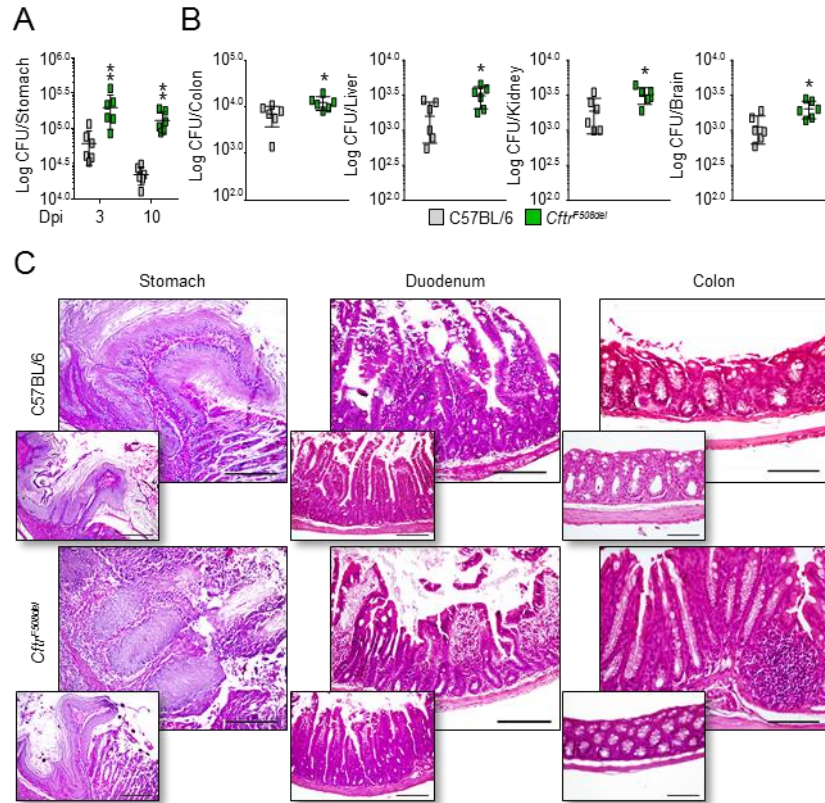


**Figure S5, related to Figure 7. *Cfr*<sup>508del</sup> mice are highly susceptible to *C. albicans* gastrointestinal infection.** C57BL/6 and *Cfr*<sup>F508del</sup> mice ( $n=6$ ) were infected intragastrically with *C. albicans* and evaluated for (A) stomach fungal growth ( $\log_{10}$  CFU, mean  $\pm$  SD), (B) dissemination in the indicated organs 3 days after infection and (C) inflammatory pathology in the stomach, duodenum and colon of infected mice at 10 dpi. Insets, uninfected mice. Photographs were taken with a high-resolution microscope (Olympus DP71). Scale bars 500  $\mu$ m and 200  $\mu$ m. \* $P < 0.05$ , \*\* $P < 0.01$ , *Cfr*<sup>F508del</sup> vs C57BL/6. Unpaired T test or two-way ANOVA, Bonferroni post test. Data represent pooled results or representative images from three experiments. Dpi, days post infection.

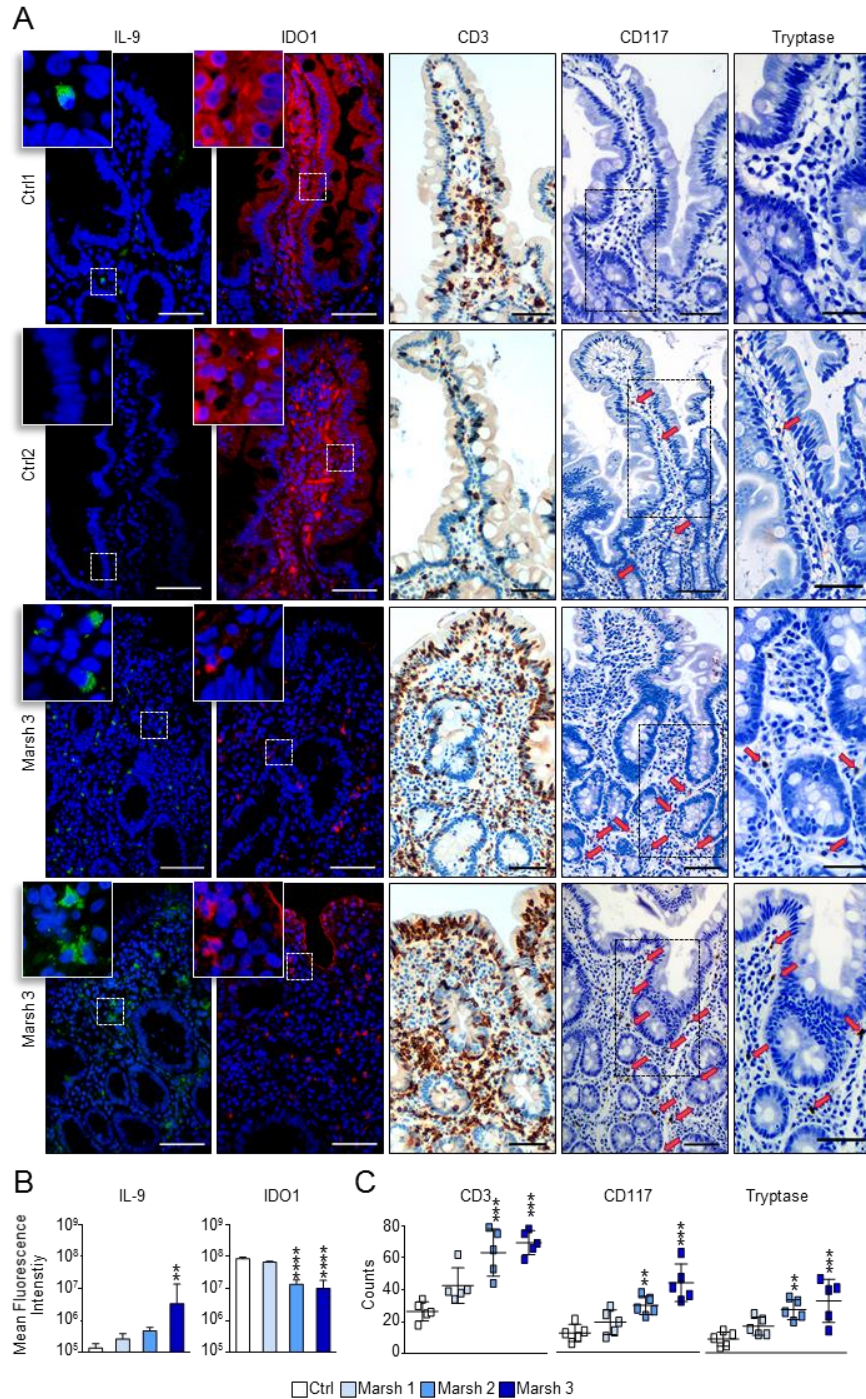


**Figure S6, related to Figure 7. IL-9/MMC are expanded in human CD.** (A) IL-9 and IDO1 protein expression by immunofluorescence, detection of CD3<sup>+</sup>, CD117<sup>+</sup> and Tryptase<sup>+</sup> cells by immunohistochemical staining in duodenal biopsies from patients with Marsh 3 scores and controls (Ctrl). (B) Relative IL-9 and IDO1 fluorescence intensity and (C) association between cell count and Marsh score. Each symbol in graphs represents the cell count average of a single subject. Photographs were taken with a high-resolution microscope (Olympus DP71). Scale bars 200  $\mu$ m and 100  $\mu$ m. IL-9 and IDO1 fluorescence intensity was measured with the ImageJ software. Data are expressed as mean  $\pm$  SD. \*\*P<0.01, \*\*\*P<0.001, Marsh 3 vs Ctrl. One- and two-way ANOVA, Tukey's and Bonferroni post test.

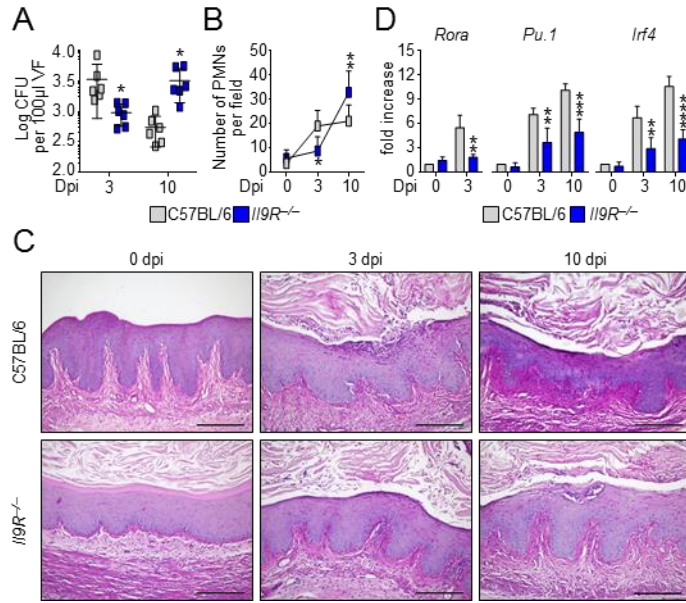


**Figure S7, related to Figure 1. Susceptibility of *Il9R*<sup>-/-</sup> mice to vaginal candidiasis.** C57BL/6 and *Il9R*<sup>-/-</sup> mice ( $n=6$ ) were intravaginally inoculated with  $5 \times 10^6$  *C. albicans* blastoconidia and assessed for (A) vaginal fungal burden ( $\text{Log}_{10}$  CFU/100µl VF  $\pm$  SD), (B) PMNs quantification in VF, (C) vaginal pathology (periodic acid-Schiff staining) and (D) ILC2 and Th9 specific transcripts gene expression in vaginal cells and purified CD4<sup>+</sup> T cells from inguinal lymph nodes respectively. Photographs were taken with a high-resolution microscope (Olympus DP71). Scale bar 100 µm. Gene expression was determined by RT-PCR. Data are expressed as mean  $\pm$  SD. \* $P < 0.05$ , \*\* $P < 0.01$ , \*\*\* $P < 0.001$ , \*\*\*\* $P < 0.0001$ , *Il9R*<sup>-/-</sup> vs C57BL/6 mice. Two-way ANOVA, Bonferroni post test. Data represent pooled results or representative images from three experiments. Dpi, days post infection. VF, vaginal fluids.